

NILU : OR 82/86
REFERENCE: O-8515
DATE : JUNE 1987
ISBN : 82-7247-762-9

A MODEL FOR LONG RANGE TRANSPORT OF SULPHUR
DIOXIDE AND PARTICULATE SULPHATE IN THE ATMOSPHERE
- A TECHNICAL DESCRIPTION

Trond Iversen*

*Present affiliation:

The Norwegian Meteorological Institute
P.O. Box 43, Blindern, N-0313 Oslo 3
Norway

NORWEGIAN INSTITUTE FOR AIR RESEARCH
P.O.BOX 64, N-2001 LILLESTRØM
NORWAY

PREFACE

The work presented in this report was financed by British Petroleum Ltd. (BP), as a part of a research programme on long range transport of air pollutants to the Norwegian Arctic.

SUMMARY

In this report is documented the methods used in a long range transport model, constructed to simulate atmospheric transport into the Arctic. The model uses isentropic surfaces as coordinate surfaces, consists of three or more layers chosen optionally, and applies a grid with spatially fixed points (eulerian). The horizontal and vertical transport is computed by an antidiffusively corrected, upwind scheme. Linear oxidation of sulphur dioxide to particulate sulphate is included, with reaction rate depending on latitude and season. Furthermore, vertical, turbulent diffusion including dry deposition, is taken into account, and the dry deposition of sulphur dioxide is assumed smaller on snow and ice than elsewhere. Precipitation scavenging is taken into account in a three-dimensional manner. Finally, the emissions are assumed mixed vertically depending on local stability. The model includes a meteorological "preprocessor" which estimates heating and precipitation from analyses of wind, massfield and humidity.

CONTENTS

	Page
PREFACE	1
SUMMARY	3
1 INTRODUCTION	7
2 BASIC EQUATIONS	8
2.1 Emissions	10
2.2 Chemistry	12
2.3 Precipitation scavenging	12
2.4 Vertical turbulent diffusion	15
3 NUMERICAL APPROXIMATIONS	17
3.1 The grid system	17
3.2 The horizontal transport	19
3.3 The vertical transport	23
3.4 Physical and chemical terms	24
3.5 The time-stepping procedure	27
3.6 Coordinate surfaces intersecting the ground	28
4 METEOROLOGICAL DATA	29
4.1 Wind and massfield	30
4.2 The surface functions	35
4.3 Diabatic heating and precipitation	37
4.3.1 Boundary layer processes	38
4.3.2 Convective precipitation	41
4.3.3 Stratiform precipitation	44
4.3.4 Terrestrial radiation	47
4.4 Choice of isentropic surfaces	53
5 PROGRAMME STRUCTURE	57
6 REFERENCES	60

A MODEL FOR LONG RANGE TRANSPORT OF SULPHUR DIOXIDE AND PARTICULATE SULPHATE IN THE ATMOSPHERE - A TECHNICAL DESCRIPTION

1 INTRODUCTION

The OECD programme on long range transport of air pollutants conducted by the Norwegian Institute for Air Research (NILU), contributed with one of the first calculated estimates of long range transported sulphur dioxide and particulate sulphate on a daily basis (OECD, 1979). This model was of the Lagrangian type, in which horizontal finite differences are not used when calculating the horizontal transport (Eliassen and Saltbones, 1975). Thus computational diffusion was avoided. On the other hand, the accuracy of the transport depended on the estimation of air parcel trajectories which accumulates the error. Furthermore, the method is applicable in practice only in models with one layer in the vertical. If the aim is to model deep tropospheric dispersion and processes influencing concentrations, several layers in the vertical must be used. Examples of eulerian models (with fixed grid points) which apply schemes for the horizontal transport with reduced computational dispersion, are several. One example is the pseudospectral method (Fox and Orzag, 1973; Christensen and Prahm, 1976), which when used together with a three-level time-integration scheme, totally removes artificial diffusion.

The present model was made for the purpose of studying the long range transport to the Arctic. Arctic air pollution of anthropogenic origins has been documented during recent years (AGASP, 1984; Arctic Air Chemistry, 1985) both on the ground and in the high troposphere. As a consequence, the model has been made with several (at least three) layers, and an Eulerian scheme is applied. As vertical coordinate, entropy (as measured by the potential temperature) is used in stead of height. The reason for this is that the change of entropy for the individual air parcels is a very slow process in large scale atmospheric flows. It is mainly in precipitation areas that the heating is of particular importance. By choosing isentropic coordinate surfaces the vertical advection is much smaller than when using horizontal surfaces.

In addition, the isentropic surfaces normally form small inclination angles with discontinuity-surfaces (fronts) in the troposphere. Gradients along isentropic surfaces will therefore often be much smaller than gradients along horizontal surfaces, and in consequence also the errors in computing the horizontal transport will be reduced.

This report is a documentation of the methods used for the model, and no results are shown. The model programme has been written in standard FORTRAN 77 for application on a ND-560 CX computer. This version of the model uses input of hemispheric meteorological analyses from National Center for Atmospheric Research, USA. The model coding has been written in a way that makes changes feasible.

2 BASIC EQUATIONS

The purpose of the model is to calculate the concentrations of sulphur dioxide and particulate sulphate. To simulate the detailed chemistry of oxidation of sulphur dioxide would require knowledge of a large amount of species as well as the microphysics of clouds (e.g. Rohde and Isaksen, 1980; Bøhler and Isaksen, 1984). Such a complicated three-dimensional model is not possible with the presently available computer equipment at NILU (ND 560-CX). As a consequence, the sulphur chemistry is treated in a simplified way, by a linear process (OECD, 1979; Eliassen and Saltbones, 1983) and two differential equations for the two concentrations are arrived at.

As advocated in the introduction, isentropic surfaces will be used as coordinate surfaces in the model (i.e. entropy, or a parameter which is a monotonic function of entropy, is the vertical coordinate). The governing equations can be written.

$$q_t = - \nabla \cdot (\vec{v}q) - (\dot{e}q)_e - [q_t]_E - [q_t]_S + Q - k_c q \quad (2.1)$$

$$s_t = - \nabla \cdot (\vec{v}s) - (\dot{e}s)_e - [s_t]_E - [s_t]_S + S + k_c q \quad (2.2)$$

The following symbols are used:

Independent variables;

- x, y : horizontal cartesian coordinates,
 e : potential temperature (entropy $\sim \log e$). By definition
 $e = T(p_r/p)^{R/c_p}$, where T is absolute temperature, p is pressure,
 $p_r = 1000$ hPa, $R = 287$ J/kg K and $c_p = 1004$ J/kg K,
 t : time,

Dependent variables

- q : concentration (mass per volume) of sulphur dioxide measured as mass of sulphur per volume,
 s : concentration of particulate sulphate measured as mass of sulphur per volume,
 \vec{v} : horizontal wind velocity,
 u, v : x and y components of \vec{v} ,
 \dot{e} : diabatic heating (vertical velocity in e -coordinates),
 $[]_E$: indicates effects of turbulent (eddy) diffusion,
 $[]_S$: indicates effects of precipitation scavenging,
 Q : emission intensity of sulphur dioxide,
 S : emission intensity of particulate sulphate,
 k_c : rate of transformation from sulphur dioxide to particulate sulphate,

Differentiation symbols;

Subscript $x, y,$

- e or t : partial derivative with respect to x, y, e or t ,
 ∇ : horizontal gradient operator ($\nabla = \vec{i}(\)_x + \vec{j}(\)_y$, where \vec{i} and \vec{j} are unit vectors in the x - and y -directions respectively.

The boundary conditions are

$$q = q_{AMB} \text{ and } s = s_{AMB} \quad (2.3)$$

at the "top" of the atmosphere $e = e_T$, where e_T is a sufficiently high value of e , above the uppermost layer in the model. The subscript

"AMB" signifies ambient air concentrations (~ 0). At the lateral boundaries a similar procedure is used by applying (2.3) at an extra grid line on the outside of the integration domain. At outflow, the concentrations are thus permitted to smoothly move out of the domain, while at inflow the ambient air concentrations are advected into the region.

The lower boundary conditions are supposed to apply at the top of the surface boundary layer. This surface is assumed to be impenetrable by large scale atmospheric transport. Turbulent diffusion is the only process causing air transport through it. Consequently, the differential equations for the concentrations at the top of the surface boundary layer can be written:

$$q_{st} = -\nabla \cdot (\vec{v}q_s) - [q_{st}]_E - [q_{st}]_S + Q_s - k_c q_s \quad (2.4)$$

$$s_{st} = -\nabla \cdot (\vec{v}s_s) - [s_{st}]_E - [s_{st}]_S + S_s + k_c q_s, \quad (2.5)$$

where subscript s signifies values at the top of the surface boundary layer where $e = e_s(x, y, t)$.

2.1 EMISSIONS

Emission surveys for sulphur dioxide has been worked out for a major part of the northern hemisphere (Semb, 1985). The estimated emission is given in terms of emitted sulphur per year and grid square in a cartesian grid system on a polar-stereographic projection of the sphere, which has a true scale factor at $60^\circ N$. The source intensity within a grid square is supposed to be evenly distributed in the horizontal, and decreases with height above the ground. The local mixing height determines the source intensity distribution in the vertical.

Let I denote the emission intensity (mass of sulphur per time) inside a grid square. A part α is assumed to be deposited locally within the grid square, and thus is not contributing to long range transport. A part β is assumed to be emitted directly as sulphate (or transformed to sulphate within the grid square), while the remaining is emitted to SO_2 .

If A denotes the grid square area and z_m the local mixing height, the rate of change of the concentrations due to emissions are

$$Q = (1 - \alpha - \beta) \frac{I}{z_m \cdot A} \cdot W(z) \quad (2.6)$$

$$S = \beta \cdot \frac{I}{z_m \cdot A} \cdot W(z)$$

where $W(z)$ is a normalized weight function of height above the ground. The chosen function is

$$W(z) = \begin{cases} 0 & ; z \geq 2z_m \\ \frac{1}{2} \cdot \left[\left(1 - \frac{z}{z_m}\right)^{1/n} + 1 \right] & ; 0 \leq z < 2z_m \end{cases} \quad (2.7)$$

with $n = 25$ (see Figure 2.1). To compute the contribution from local

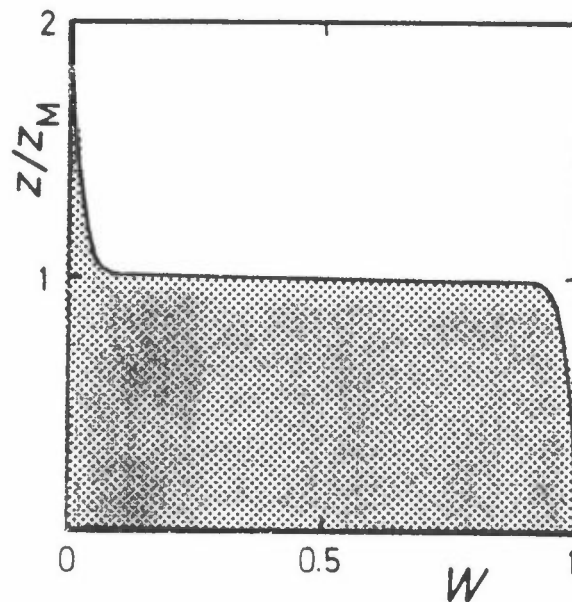


Figure 2.1: The weight function W for the vertical distribution of source strength.

emissions to the concentration in an isentropic surface, the height of the surface above ground has to be known. Since $W(0) = 1$, then

$$Q_S = (1 - \alpha - \beta) \frac{I}{z_m \cdot A} \quad \text{and} \quad S_S = \beta \frac{I}{z_m \cdot A}.$$

The grid square area is

$$A = (d/m)^2 \quad (2.8)$$

where d is the mesh size at 60°N and m is the map factor

$$m = (1 + \sin B_0)/(1 + \sin B) \quad (2.9)$$

where $B_0 = 60^\circ$ and B is the latitude.

2.2 CHEMISTRY

As seen from the governing equations, the sulphur chemistry is treated in a simplified manner by linear terms. The oxidation factor k_c is assumed to depend on received sunlight. Hence, it is made dependent of the latitude, with coefficients varying with the season of the year:

$$k_c = (k_{c,ekv} - k_{c,pole}) \frac{r}{R} + k_{c,pole} \quad (2.10)$$

where r is a point's distance from the north pole in map coordinates and R is the corresponding distance between the equator and the north pole. The values of $k_{c,ekv}$ and $k_{c,pole}$ can be chosen to vary with season. It seems reasonable to assume that the seasonal variation at the pole is more significant than at the equator.

2.3 PRECIPITATION SCAVENGING

In the real atmosphere, precipitation scavenging of SO_2 and sulphate involves a complicate system of physico-chemical processes on the micro-scale. As for the gas-phase oxidation process, a simplified treatment is used in the present model.

If c denotes either q or s and F_w is the downward flux density of c due to precipitation scavenging, then

$$- [c_t]_S = \frac{\partial F_w}{\partial z} \quad (2.11)$$

The present scheme distinguishes between "rainout" and "washout". In layers where precipitation is created, there is a possibility to use a scavenging efficiency different from the one used in layers where the precipitation is falling passively. This is especially important for sulphate, since sulphate particles are hygroscopic and thus are active cloud-physical elements.

Let $P(z)$ denote the flux density of precipitation mass that falls through any level z in the atmosphere (mass of H_2O per horizontal area and time). If $dP/dz < 0$ at a level z , it is assumed that this level is inside a precipitating cloud. If $dP/dz = 0$ and $P > 0$, precipitation is falling through the atmosphere (see Figure 2.2).

Knowledge of the air concentration c and the precipitation intensity P , is not sufficient to calculate the flux density F_w . A relation between the concentration in air c and concentration in precipitation c_w is therefore assumed. The air concentration is assumed to influence the vertical gradient of c_w by

$$\frac{dc_w}{dz} = - \mu c \quad (2.12)$$

where μ is called the scavenging efficiency. This factor should parameterize all the physico-chemical processes involved, and the following rather crude estimate is applied.

$$\mu = \frac{W}{h} \quad (2.13)$$

where W is the scavenging ratio (e.g. Barrie, 1981) and h is a mean effective scavenging depth. This corresponds to the method used by Eliassen and Saltbones (1983) in their "experimental model".

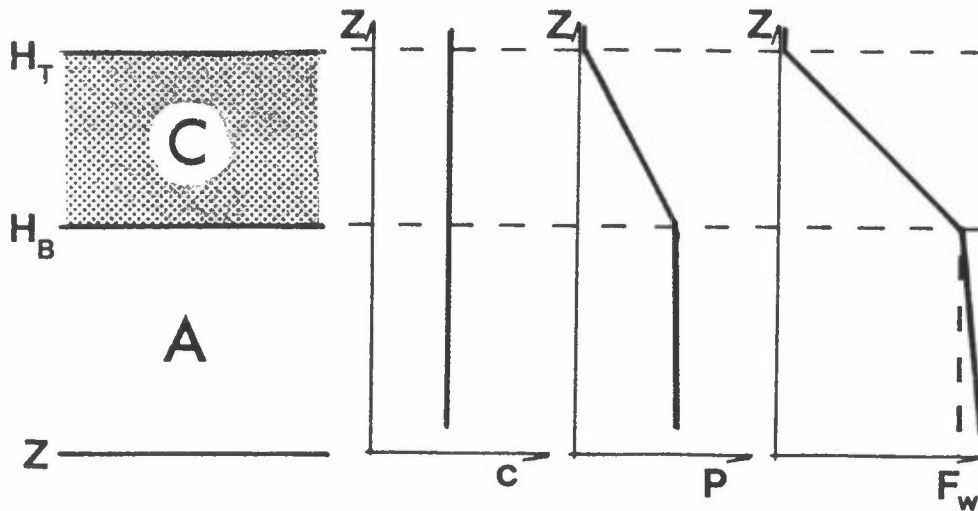


Figure 2.2: Precipitation scavenging. C = cloudy air, A = unsaturated air. The downward flux density of sulphur F_w is shown for a choice of air concentration c and precipitation intensity P .

Let subscript A denote unsaturated air and C cloud-air. Supposing a precipitating cloud in the layer $[H_B, H_T]$ (see Figure 2.2), the contribution to the flux density F_w at a level z from the precipitation produced in the cloud is:

$$F_w^k(z) = \frac{1}{\rho_w} \cdot \begin{cases} 0 & ; z > H_T \\ W_C \int_z^{H_T} (-c) \delta \zeta \cdot \int_z^{H_T} (dP/d\zeta) \delta \zeta & ; H_T > z \geq H_B \\ [W_C \int_{H_B}^{H_T} (-c) \delta \zeta + W_A \int_z^{H_B} (-c) \delta \zeta] \cdot \int_{H_B}^{H_T} (dP/d\zeta) \delta \zeta & ; z < H_B \end{cases} \quad (2.14)$$

Here ρ_w is the density of the precipitating matter, and the superscript k indicates that this is the contribution from a cloud no. k in the total column. Hence the total flux density at level z is:

$$F_w(z) = \sum_{k=1}^K F_w^k(z) \quad (2.15)$$

where K is the number of cloud layers above the level z . The wet deposition rate per unit area to the ground is then

$$D_{\text{wet}} = F_w(0) \quad (2.16)$$

2.4 VERTICAL TURBULENT DIFFUSION

The isentropic surfaces are in general only permeable by air parcels which are losing or gaining internal energy through diabatic heating. However, since the meteorological information for this model is on a very large scale, there may be transport through these surfaces due to small scale motion. This is especially important in the planetary boundary layer, and when there is low static stability.

If c denotes either q or s , then

$$-[c_t]_E = F_e/z_e = F_z \quad (2.17)$$

where F is the turbulent flux density. The quantity is approximated by

$$F = \begin{cases} Kc_e & ; z > H_s \\ v_d c & ; z \leq H_s \end{cases} \quad (2.18)$$

where K is the exchange coefficient, v_d is the dry deposition speed and H_s is the height of the turbulent surface layer. The flux density $F = v_d c$ is constant in the surface layer.

Normally, the value of v_d is given for a height close the ground, e.g. $z = 1$ m. However, we do not know the corresponding concentration from the governing equations. Eqs. (2.4) and (2.5) give c_s which is supposed to be the concentration at $z = H_s$. The flux density in the surface may be written

$$F = C_H |\vec{v}| (c - c_G) \quad (2.19)$$

where C_H can be calculated from Monin-Obhukov theory by the use of the Louis (1979) - functions (see Ch. 4). The dry deposition speed at the top of the surface layer can then be written

$$v_{ds} = \frac{v_{dG}}{1 + v_{dG}/(C_H |\vec{v}_s|)} \quad (2.20)$$

where the subscript s denotes values at top of the surface layer and the subscript G denotes values at about 1 m. The concentration at $z = 1$ m, is

$$c_G = c_s [1 - v_{ds} / (C_H |\vec{v}_s|)] \quad (2.21)$$

The vertical exchange coefficient above the surface layer is determined by the formula

$$K = \begin{cases} 0 & ; Ri > Ri_c \\ (1 - Ri/Ri_c) K_{max} & ; 0 < Ri < Ri_c \\ K_{max} & ; Ri < 0 \end{cases} \quad (2.22)$$

where the Richardson number is

$$Ri = \frac{g}{\theta} \frac{\partial \theta / \partial z}{|\partial \vec{v} / \partial z|^2} \quad (2.23)$$

and the critical Richardson number determines the initiation of turbulence. The present choice is

$$Ri_c = 1 \quad (2.24)$$

When using isentropic coordinate surfaces, it is a priori assumed that the atmosphere is stable. In the real atmosphere unstable layers may occur, especially in the boundary layer. The a priori assumption is taken into account when calculating Ri, by letting the stability parameter be

$$\frac{\partial \theta}{\partial z} = \frac{1}{z_\theta} - (\theta_z)_{min} \quad (2.25)$$

where z_θ is computed in a straight forward manner in θ -coordinates and $(\theta_z)_{min} = 2 \cdot 10^{-3} \text{ Km}^{-1}$.

The maximum exchange coefficient K_{max} is made dependent on the vertical discretization, and is exactly the value needed for total mixing over one timestep.

The dry deposition rate per unit area is

$$D_{dry} = F_s = v_{ds} c_s \quad (2.26)$$

3 NUMERICAL APPROXIMATIONS

3.1 THE GRID SYSTEM

The governing equations (2.1), (2.2), (2.4) and (2.5) must be approximated in order to be solved numerically. To approximate derivatives the method of finite difference has been chosen. The equations are solved on a polar-stereographic map with map factor given by Eq. (2.9). The horizontal grid mesh consists of squares with sides of true length ≈ 300 km at $B_0 = 60^\circ N$. All variables are defined in common grid points. The meridian $L_0 = 32^\circ W$ is parallel to the grid lines in the y-direction. Figure 3.1 shows the horizontal grid system applied for simulations so far.

The vertical discretization is troublesome when using coordinate surfaces that may not exist in all grid points. The isentropic surfaces should be chosen so that at any place and time during the simulations, at least two of them exist in the real atmosphere. Suppose that there has been chosen a set of L isentropic surfaces in addition to the ground surface, in which the sulphur concentrations are to be computed. Thus, in a point (x,y) c (being either q or s) is computed for $e = e_S(x,y)$ and for $e \in \{e_1, \dots, e_M\}$ where $M \leq L$. The lowermost isentropic surface e is defined such that

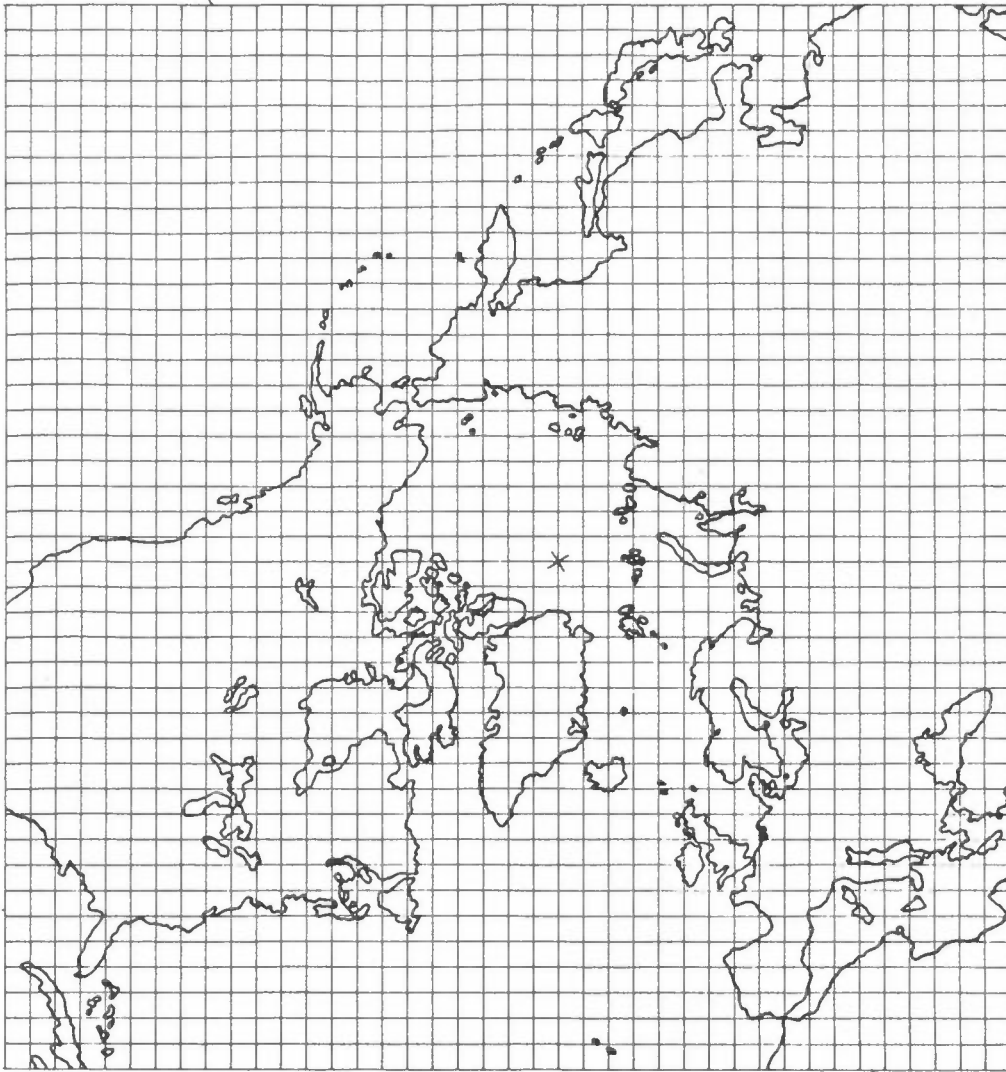


Figure 3.1: An example of horizontal grid system on a polar stereographic map.

$$\theta_M \geq \theta_S(x, y) + \varepsilon$$

and when $M < L$:

(3.1)

$$\theta_{M+1} < \theta_S(x, y) + \varepsilon$$

where the term $\varepsilon = 1K$. Gridpoints where $\theta \in \{\theta_{M+1}, \dots, \theta_L\}$ are called extraordinary points (Eliassen and Hellevik, 1975). The isentropic surfaces must be chosen such that $M \geq 2$ for any (x, y) . In computing

terms involving differentiation with respect to e , a staggered vertical grid is chosen, see Figure 3.2.

Thus, $\hat{e}_\iota = e_\iota$ for $\iota = 1, \dots, M$, $\hat{e}_0 = 2e_1 - e_2$, $\hat{e}_{M+1} = e_S(x, y)$ and $\hat{e}_{\iota+1/2} = (\hat{e}_\iota + \hat{e}_{\iota+1})/2$ for $\iota = 0, \dots, M$.

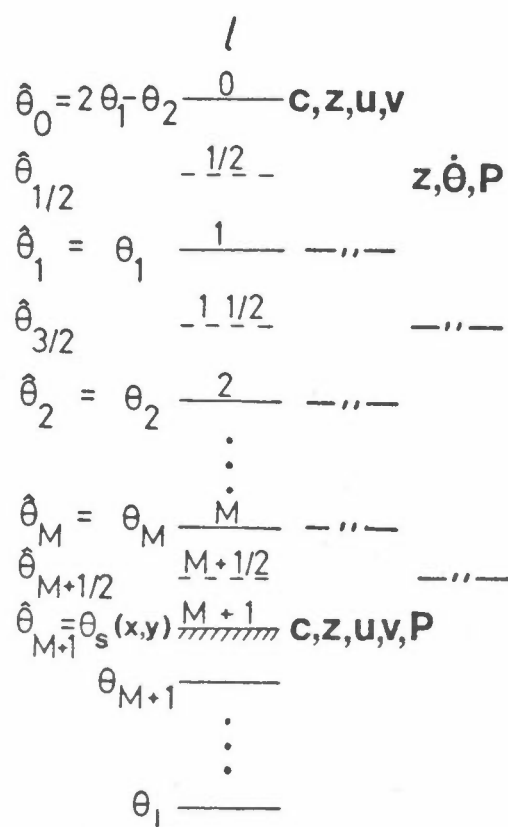


Figure 3.2: Sketch of information levels in a point (x, y) .

3.2 THE HORIZONTAL TRANSPORT

The main problem with Eulerian dispersion models is the computation of the horizontal transport. Several methods have been proposed in the literature, and for the present model a method introduced by Smolarkiewicz (1983) is employed.

The horizontal transport is the differential, horizontal flux of concentration:

$$[c_t]_H = - m^2 \nabla \cdot (\vec{v}c/m) = - m^2 [(cu/m)_x + (cv/m)_y] \quad (3.2)$$

By applying the Marchuk splitting technique (Mesinger and Arakawa, 1976, p. 58) the x-component and y-component can be treated separately. Here, the treatment of the x-component is shown, the y-component being treated analogously. Since the scheme is originally designed for a staggered grid where u is defined at gridpoints halfway between those where c are defined, let

$$u_{i+1/2}^n = \left(\frac{u_i^n}{m_i} + \frac{u_{i+1}^n}{m_{i+1}} \right) / 2 \quad (3.3)$$

where i is gridpoint no. i in the x-direction, and n is the time level number. By defining

$$G(c_i, c_{i+1}, u) = m_i^2 \frac{\Delta t}{2d} [(u+|u|)c_i + (u-|u|)c_{i+1}], \quad (3.4)$$

a standard upwind approximation to the x-component is

$$w_i^1 = c_i^n - [G(c_i^n, c_{i+1}^n, u_{i+1/2}^n) - G(c_{i-1}^n, c_i^n, u_{i-1/2}^n)] \quad (3.5)$$

where w_i^1 is the first approximation to c_i^{n+1} due to the x-component. The timestep length is Δt . The upwind scheme has the favourable property of being positive definite; if all c_i are positive at one timelevel, then their upwind approximation for the next timelevel are also positive. Hence no spurious wavelike solutions are created. On the other hand, the upwind scheme implicitly introduces a horizontal diffusion which is intolerably large. The new method introduced by Smolarkiewicz (1983) reverses the effect of the implied computational diffusion by defining an antidiffusive wind velocity for e.g. (3.5) The procedure may be repeated a number of iterations. Thus define

$$\tilde{u}_{i+1/2}^v = \frac{[|\tilde{u}_{i+1/2}^{v-1}|d - \Delta t (\tilde{u}_{i+1/2}^{v-1})^2] \cdot (w_{i+1}^{v-1} - w_i^{v-1})}{(w_i^{v-1} + w_{i+1}^{v-1} + \xi) d} \quad (3.6)$$

for $v = 2, 3, \dots$ and $\tilde{u}_{i+1/2}^1 = u_{i+1/2}^n$. The term ξ is to assure a non-zero denominator; $\xi = 10^{-15}$. Then approximation no. v is

$$w_i^v = w_i^{v-1} - [G(w_i^{v-1}, w_{i+1}^{v-1}, \tilde{u}_{i+1/2}^v) - G(w_{i-1}^{v-1}, w_i^{v-1}, \tilde{u}_{i-1/2}^v)] \quad (3.7)$$

for $v = 2, 3, \dots$

In simulations performed so far, five iterations are performed, i.e.

$$[c_i^{n+1}]_{HX} = w_i^6, \quad (3.8)$$

where HX signifies the x-component of the horizontal transport. Figure 3.3 shows results for one-dimensional tests with different number of iterations.

The stability requirement for the total scheme is the same as for the pure upwind scheme:

$$\max \left\{ \frac{|u_{i+1/2}^n| \Delta t}{d} \right\} \leq 1 \quad (3.9)$$

By combining with the y-component by the Marchuk splitting method, a sufficient stability requirement is

$$\max \left\{ |u_{i+1/2,j}^n| \cdot |v_{i,j+1/2}^n| \frac{\Delta t^2}{d^2} \right\} \leq 1. \quad (3.10)$$

If the x- and y-components are stable separately, then the combination is stable.

The horizontal flux can be written

$$m^2 \vec{v} \cdot (\vec{v}c/m) = m^2 c \vec{v} \cdot (\vec{v}/m) + m \vec{v} \cdot \nabla c. \quad (3.11)$$

It is thus seen that the term consists of two effects; divergence and advection. In general, large scale atmospheric flows divergence are at least one order of magnitude smaller than advection. Since the divergence is very difficult to analyse correctly from observations of wind, the possibility to discard the divergence term and only compute the advection has been included as an option. The first step in the iteration procedure, the upwind scheme, is then changed from (3.5) to

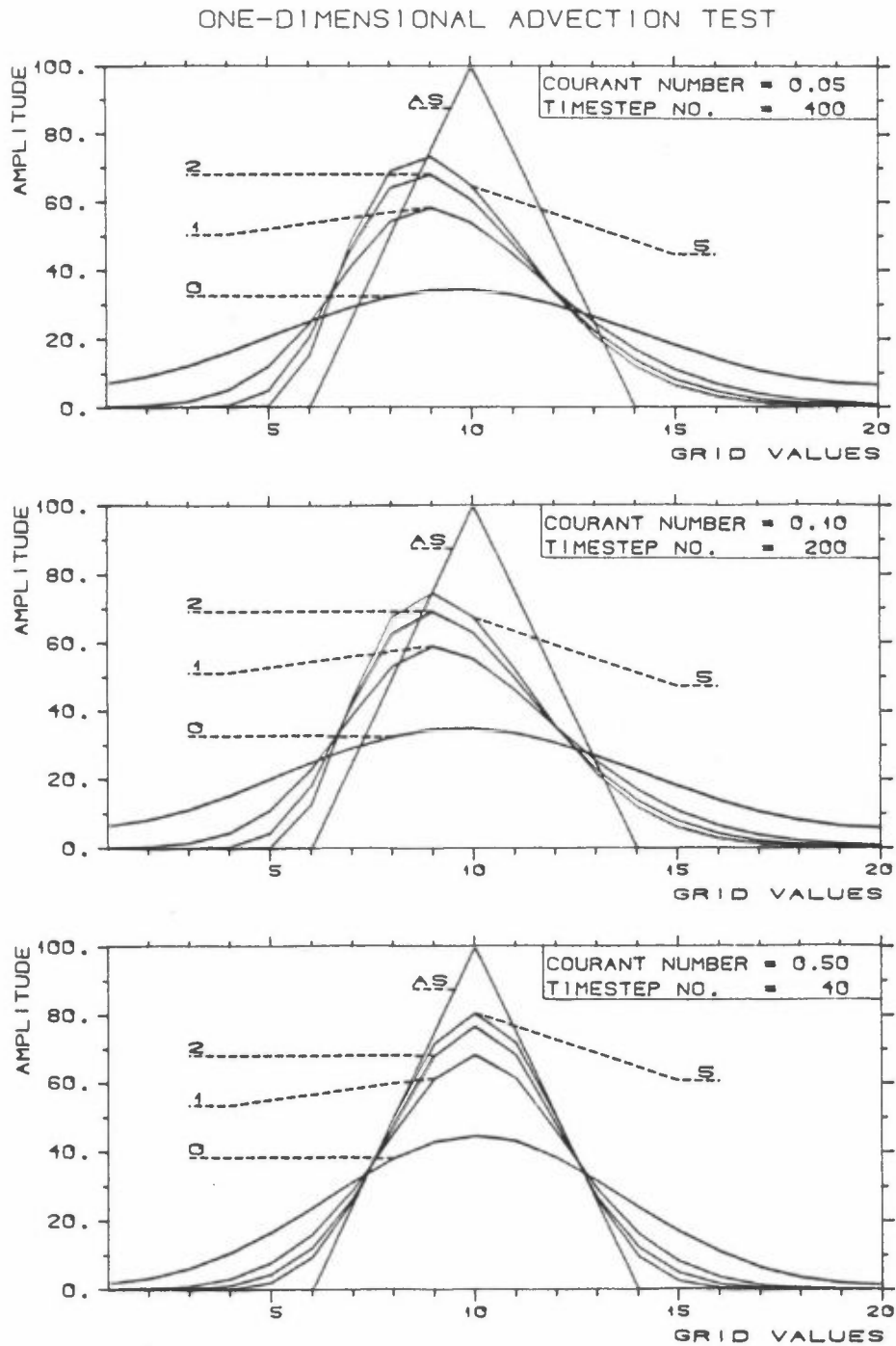


Figure 3.3: Examples of application of horizontal transport scheme with constant wind U in one dimension. The Courant number $= U\Delta t/\Delta x$ (Δt = timestep length, Δx = grid resolution) was assumed three different values. The diagrams show analytical solution (AS), and results from scheme with 0,1,2 and 5 iterations with antidiffusive corrections.

$$w_i^1 = c_i^n - m \frac{\Delta t}{2d} [(u_i^n + |u_i^n|) (c_i^n - c_{i-1}^n) + (u_i^n - |u_i^n|) (c_{i+1}^n - c_i^n)] \quad (3.12)$$

The corrective steps are made as before, eqs. (3.6) and (3.7).

3.3 THE VERTICAL TRANSPORT

The vertical transport through the isentropic surfaces is due to diabatic heating/cooling of air parcels. The vertical "velocity" is denoted by ϵ which is the rate of change of potential temperature for individual air parcels. The vertical flux term is

$$[c_t]_v = - (\dot{\epsilon} c)_\epsilon \quad (3.13)$$

The method by Smolarkiewicz (1983) is applied also to compute this term. Following the notation of Figure 3.2, define

$$\text{and } \left. \begin{array}{l} \Delta\theta_{\iota-1/2} = \hat{\theta}_{\iota-1} - \hat{\theta}_{\iota} ; \\ \Delta\theta_{\iota} = \hat{\theta}_{\iota-1/2} - \hat{\theta}_{\iota+1/2} \end{array} \right\} \iota = 1, \dots, M \quad (3.14)$$

The method is then for $\iota = 1, \dots, M$ and $v = 1, 2, \dots$

$$w_{\iota}^v = w_{\iota}^{v-1} - \frac{\Delta t}{2\Delta\theta_{\iota}} \cdot [(\tilde{\epsilon}_{\iota+1/2}^v + |\tilde{\epsilon}_{\iota+1/2}^v|) w_{\iota}^{v-1} + (\tilde{\epsilon}_{\iota+1/2}^v - |\tilde{\epsilon}_{\iota+1/2}^v|) w_{\iota-1}^{v-1} - (\tilde{\epsilon}_{\iota+1/2}^v + |\tilde{\epsilon}_{\iota+1/2}^v|) w_{\iota-1}^{v-1} - (\tilde{\epsilon}_{\iota+1/2}^v - |\tilde{\epsilon}_{\iota+1/2}^v|) w_{\iota}^{v-1}], \quad (3.15)$$

where for $\iota = 0, \dots, M$ and $v = 2, 3, \dots$

$$\tilde{\epsilon}_{\iota+1/2}^v = \frac{[|\tilde{\epsilon}_{\iota+1/2}^{v-1}| \Delta\theta_{\iota+1/2} - \Delta t \cdot (\tilde{\epsilon}_{\iota+1/2}^{v-1})^2] (w_{\iota+1}^{v-1} - w_{\iota}^{v-1})}{(w_{\iota}^{v-1} + w_{\iota+1}^{v-1} + \xi) \Delta\theta_{\iota+1/2}} \quad (3.16)$$

Initial conditions are $w_{\iota}^0 = c_{\iota}^n$ and $\tilde{\epsilon}_{\iota+1/2}^{v=1} = -\dot{\epsilon}_{\iota+1/2}^n$ (the minus sign is necessary since ι increases in the opposite direction than ϵ). Also here, five iterations are run so that

$$[c_{\iota}^{n+1}]_v = w_{\iota}^6 \quad (3.17)$$

The stability requirement is

$$\max \left\{ \frac{|\dot{\theta}_{\iota+1/2}^n| \Delta t}{\Delta \theta_{\iota}} \right\} \leq 1, \quad (3.18)$$

which normally is a much weaker condition than (3.10).

3.4 PHYSICAL AND CHEMICAL TERMS

The source terms Q and S in the governing equations are calculated in a straightforward manner from (2.6) at the levels where the concentrations c are computed:

$$\left. \begin{aligned} Q_{\iota} &= (1-\alpha-\beta) \frac{I}{z_m A} \cdot W(z_{\iota}) \\ \text{and} \\ S_{\iota} &= \beta \frac{I}{z_m A} W(z_{\iota}) \end{aligned} \right\} \iota = 1, \dots, M+1 \quad (3.19)$$

The calculation of the oxidation factor k_c is done by (2.10) where r and R are measured with the grid constant d as unit. The grid shown in Figure 3.1 has by definition $R = 39.5$ and for a gridpoint (i, j) ,

$$r_{i,j} = [(i-i_p)^2 + (j-j_p)^2]^{1/2} \quad (3.20)$$

where (i_p, j_p) is the coordinate of the north pole, which for the actual grid is $(i_p, j_p) = (23, 21)$.

The numerical calculation of the precipitation scavenging is somewhat more laborious. The precipitation intensity is known at half-integer levels and at the surface:

$$P_{\iota+1/2} = P(z_{\iota+1/2}); \quad \iota = 0, \dots, M, M+1/2, \quad (3.21)$$

and flux densities of c_w , F , and the concentrations in precipitation are computed at the same levels. Firstly, the potential wet concentration is computed with scavenging ration W_A and W_C respectively. With the potential wet concentrations is meant what the concentration in

precipitation would have been if there were precipitation in the total column. From eqs. (2.12) - (2.13) two sequences may then be computed:

$$c_{w,A}(z_{\iota+1/2}) = c_{w,A}(z_{\iota-1/2}) + \frac{W_A}{h} c_{\iota}(z_{\iota-1/2} - z_{\iota+1/2}),$$

for $\iota = 1, 2, \dots, M+1;$ (3.22)

$$c_{w,A}(z_{1/2}) = 0,$$

where by convention $z_{M+3/2} \equiv z_{M+1} \equiv 0$. A similar formula for $c_{w,C}$ is achieved by substituting the subscript A with C in (3.22). Secondly, the flux densities F_w are computed. Suppose that there at level k is released a precipitation amount $\Delta P_k = P_{k+1/2} - P_{k-1/2}$, where $k \leq \iota$, see Figure 3.4. The contribution to the flux density $F_w(z_{\iota+1/2})$ from the pollution scavenged by ΔP_k , is:

$$F_w^k(z_{\iota+1/2}) = \frac{1}{\rho_w} [c_{w,C}(z_{k+1/2}) - c_{w,C}(z_{k-1/2}) + c_{w,A}(z_{\iota+1/2}) - c_{w,A}(z_{k+1/2})] \cdot \Delta P_k$$
 (3.23)

for $\iota = 1, \dots, M+1$ and $1 \leq k \leq \iota$

The total flux density at level $\iota+1/2$ is then by eq. (2.15):

$$F_w(z_{\iota+1/2}) = \sum_{k=1}^{\iota} F_w^k(z_{\iota+1/2}); \quad \iota = 1, 2, \dots, M+1$$
 (3.24)

It is assumed that

$$F_w(z_{1/2}) = 0$$
 (3.25)

The pollution removed from the level ι is finally computed by discretizing (2.11):

$$[c_{\iota}^{n+1}]_S = c_{\iota}^n + \Delta t \cdot [F_w(z_{\iota-1/2}) - F_w(z_{\iota+1/2})] / (z_{\iota-1/2} - z_{\iota+1/2})$$
 (3.26)

The wet deposition per unit area over the timestep Δt is

$$\Delta D_{\text{wet}} = \Delta t \cdot F_w(z_{M+1}).$$
 (3.27)

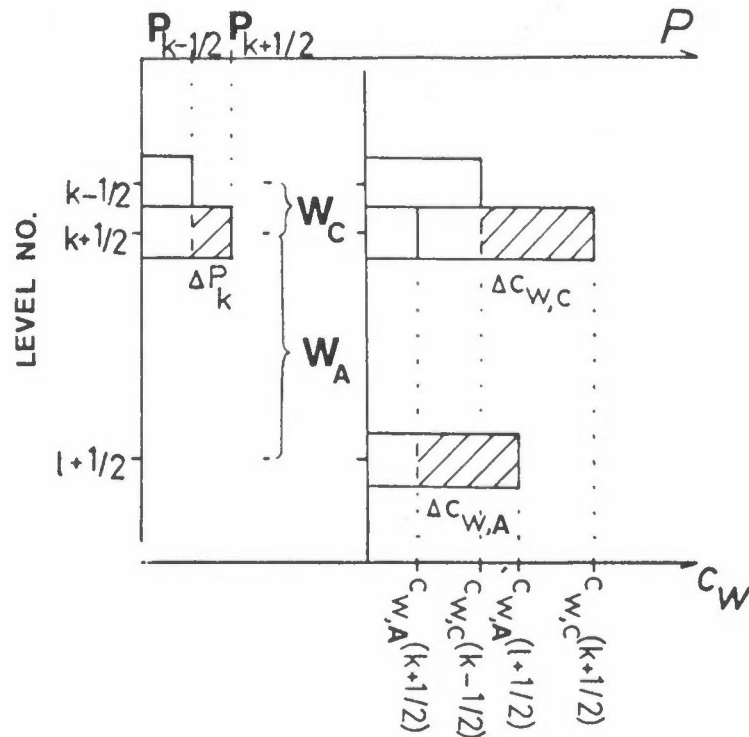


Figure 3.4: Contribution to the flux density of pollutant in precipitation at level $l+1/2$ from precipitation released at level k . The contribution is $F_w^k(l+1/2) = (\Delta c_{w,C} + \Delta c_{w,A}) \Delta P_k / e_w$.

The flux densities of pollution due to vertical, turbulent diffusion, F , is computed at the same levels as the wet flux densities F_w . At level $M+1$, which is assumed to be at the top of the surface layer, we have;

$$F(z_{M+1}) = v_{ds} \cdot c_s \quad (3.28)$$

where v_{ds} is given by eq. (2.20). At levels above, eq. (2.22) is applied. The maximum exchange coefficient is assumed to lead to total mixing between adjacent layers over one timestep Δt . Consequently

$$K_{\max}(z_{l+1/2}) = \frac{z_\theta}{\Delta t} \cdot \frac{\Delta \theta_l \cdot \Delta \theta_{l+1} \cdot \Delta \theta_{l+1/2}}{\Delta \theta_l + \Delta \theta_{l+1}}, \quad (3.23)$$

$$l = 1, 2, \dots, M.$$

By convention, $\Delta \theta_{M+1} = \theta_{M+1/2} - \theta_{M+1}$. The stability z_θ is given directly from the meteorological data (see next chapter) in the same

levels as F are computed. Having estimated K_{\max} , the actual exchange coefficient K is computed by (2.22). The Richardson's number is

$$\text{Ri}(z_{\iota+1/2}) = \frac{g}{\Delta\theta_{\iota+1/2}} \cdot \left[\frac{1}{z_{\theta}} - (\theta_z)_{\min} \right] \cdot \frac{(z_{\iota} - z_{\iota-1})^2}{(u_{\iota} - u_{\iota+1})^2 + (v_{\iota} - v_{\iota+1})^2}$$

$$; \iota = 1, \dots, M \quad (3.30)$$

where g is the acceleration of gravity, $g = 9.8 \text{ ms}^{-2}$. The flux density is then

$$F(z_{\iota+1/2}) = \begin{cases} 0 \\ K(z_{\iota+1/2}) \cdot \frac{c_{\iota} - c_{\iota+1}}{\Delta\theta_{\iota+1/2}} \end{cases} \text{ for } \iota = 0, \dots, M \quad (3.31)$$

and finally the removed pollution is computed by discretizing (2.17):

$$[c_{\iota}^{n+1}]_E = c_{\iota}^n + \Delta t \cdot \frac{F(z_{\iota-1/2}) - F(z_{\iota+1/2})}{z_{\iota-1/2} - z_{\iota+1/2}}; \iota = 1, \dots, M+1 \quad (3.32)$$

where once again by convention $z_{M+3/2} \equiv z_{M+1} \equiv 0$.

The dry deposition per unit area over the timestep Δt is

$$\Delta D_{\text{dry}} = \Delta t \cdot F(z_{M+1}) = \Delta t \cdot v_{\text{ds}} \cdot c_s \quad (3.33)$$

3.5 THE TIME-STEPPING PROCEDURE

The terms on the right hand side of the governing equations are separated into groups. The time-stepping is performed by integrating each group separately and combine them by the Marchuk splitting method. Let

$$\begin{aligned} \text{HX}(c) &= - (uc)_x \\ \text{HY}(c) &= - (uc)_y \\ \text{V}(c) &= - (\dot{\theta}c)_{\theta} \\ \text{PH}(c) &= - [c_t]_E - [c_t]_S + C + kc \end{aligned} \quad (3.34)$$

where c is either q or s , C is either Q or S and $k = -k_c$ for $c = q$ and $k = k_c$ for $c = s$. The time-stepping is then performed as follows,

$$\begin{aligned}
W^1 &= c^n + \Delta t \cdot HX(c^n) \\
W^2 &= W^1 + \Delta t \cdot HY(W^1) \\
W^3 &= W^2 + \Delta t \cdot V(W^2) \\
c^{n+1} &= W^3 + \Delta t \cdot PH(W^3)
\end{aligned}
\tag{3.35}$$

3.6 COORDINATE SURFACES INTERSECTING THE GROUND

When computing the horizontal transport terms in an isentropic surface e_l as described in section 3.2, it may happen that neighbour grid points may not exist. For example, while $e_{i,j,\iota} \geq e_s(x_i, y_j)$ the neighbour point may have $e_{i+1,j,\iota} < e_s(x_{i+1}, y_j)$, see Fig. 3.5. The values of c and \vec{v} in the point $(i+1, j, \iota)$ then have no physical meaning. However, to be able to use the formulae (3.5)-(3.8), the function in the non-existing neighbour point must be given a reasonable value, in order to estimate the horizontal transport in (i, j, ι) . Following the idea of Eliassen and Hellevik (1975), values in extraordinary points as defined by eq. (3.1) are rejected. Since the vertical gradients of wind and concentrations in the lower, planetary boundary layer usually are small, values in extraordinary points are put equal to surface values u_s , v_s and c_s . The horizontal transport may thus be approximated, though this include some wasted time to compute fictitious values in subterrain points.

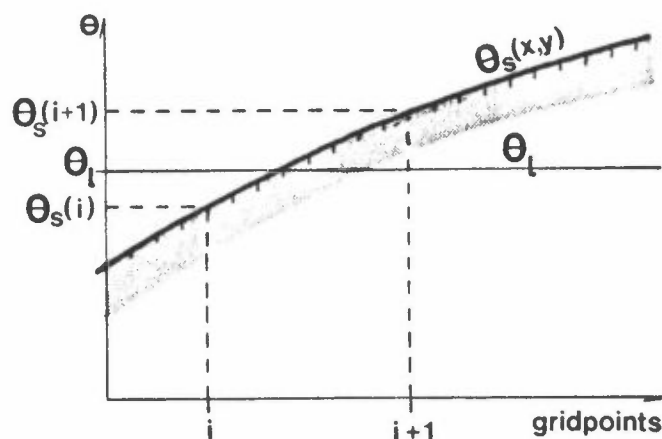


Figure 3.5: The intersection $e_l = e_s$. $e = e_l(i)$ defines a point in the atmosphere while $e_l(i+1)$ does not exist.

4 METEOROLOGICAL DATA

As seen in chapter 3, information about horizontal wind $\vec{v} = (u,v)$, geopotential height z , diabatic heating $\dot{\theta}$ and precipitation flux density P must be known at any time and in any isentropic surface ($\theta = \text{constant}$) in the atmosphere. In addition, the surface potential temperature $\theta_s(x,y)$, surface values of z , u , v and P , the surface layer bulk aerodynamic diffusion coefficient C_H and the local mixing height z_m have to be known at any time.

Analyses of z , \vec{v} and relative humidity Rh for the northern hemisphere have been obtained from the US National Center for Atmospheric Research (NCAR). The variables are given in standard pressure levels 1000 hPa, 850 hPa, 700 hPa, 500 hPa and 300 hPa (according to the recommendation of WMO, hPa is used as unit for pressure, 1 hPa = 1 mb) in a longitude-latitude grid with mesh size 2.5 degrees. The analyses have been made at main synoptic hours, 0000 and 1200 GMT. The wind components are the longitudinal u_L (positive towards the east) and the latitudinal u_B (positive towards the north).

INPUT		OUTPUT	
geographical grid		cartesian grid	
	k	p/hPa	
	1/2	200	θ, z_θ
z, u_B, u_L, Rh	1	300	$\theta, u, v, \dot{\theta}, P$
	1 1/2	400	---
---	2	500	---
	2 1/2	600	---
---	3	700	---
	3 1/2	775	---
---	4	850	---
	4 1/2	925	---
---	5	1000	---
		surface	θ, C_H, z_M

Figure 4.1: Information surfaces on input to meteorological model (NCAR-data) and on output.

To be able to calculate the data as sketched on the output side in Figure 3.2 at any time-level, a diagnostic meteorological model is

applied every twelve hours. The output from this diagnostic model must be fields in pressure levels and on the ground surface, which may be interpolated in time and used to compute the variables at isentropic surfaces. As seen from Figure 4.1 these data are the surface functions e_s , C_H and z_m ; in main pressure surfaces e , u , v , \dot{e} and P ; and in secondary pressure surfaces e and z_e . These variables are to be given in the grid points of the Cartesian grid on the polar stereographic map.

4.1 WIND AND MASSFIELD

The transformation from geographical coordinates (L, B) to Cartesian coordinates (x, y) , requires two operations. The scalar fields must be interpolated from gridpoints in the geographical grid to gridpoints (i, j) in the Cartesian grid, and the longitudinal and latitudinal wind components must be projected onto the Cartesian axes.

A Cartesian grid on a polar-stereographic map is uniquely defined by the latitude of true scale B_0 , the grid-parallel longitude L_0 , the pole-to-equator distance R measured in grid units, and the coordinates of the north pole (i_p, j_p) . The grid shown on Figure 3.1 has $B_0 = 60^\circ$, $L_0 = -32^\circ$, $R = 39.5$ and $(i_p, j_p) = (23, 21)$.

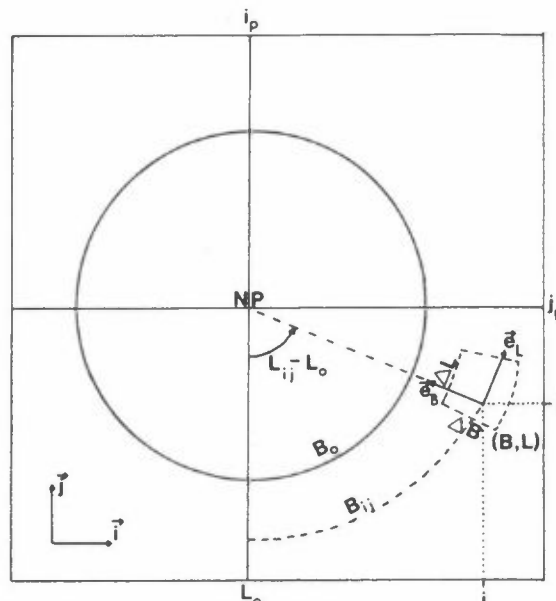


Figure 4.2: Transformation from geographical coordinates (L, B) with unit vectors (\vec{e}_L, \vec{e}_B) , to Cartesian coordinates (i, j) with unit vectors (\vec{i}, \vec{j}) . The meridian L_0 coincides with cartesian coordinate i_p . B_0 is the latitude of true scale of the map projection.

The first step in the interpolation procedure is to compute the latitude $B_{i,j}$ and longitude $L_{i,j}$ in each gridpoint (i,j) , see Figure 4.2. If the scalar h is given in geographical gridpoints with mesh size ΔB and ΔL , the one which has $B \leq B_{i,j}$ and $B + \Delta B > B_{i,j}$ is found, W and similar for L . Then by linear interpolation,

$$\begin{aligned} h_{i,j} = & \{(B+\Delta B-B_{i,j}) \cdot [(L+\Delta L-L_{i,j}) \cdot h(B,L) + (L_{i,j}-L) \cdot h(B,L+\Delta L)] \\ & + (B_{i,j}-B) \cdot [(L+\Delta L-L_{i,j}) \cdot h(B+\Delta B,L) \\ & + (L_{i,j}-L) \cdot h(B+\Delta B,L+\Delta L)]\}/\Delta L\Delta B \end{aligned} \quad (4.1)$$

The values $B_{i,j}$ and $L_{i,j}$ are given by

$$\sin B_{i,j} = (R^2 - r_{i,j}^2)/(R^2 + r_{i,j}^2) \quad (4.2)$$

where $r_{i,j}^2 = (i-i_p)^2 + (j-j_p)^2$, and

$$\sin (L_{i,j}-L_0) = (i - i_p)/r_{i,j}$$

and

$$\cos (L_{i,j}-L_0) = (j_p - j)/r_{i,j} \quad (4.3)$$

The calculation of (u,v) from (u_L, u_B) is performed by rotating the unit vectors an angle $L_0 - L$. The wind components are consequently

$$u = u_L \cos (L-L_0) - u_B \sin (L-L_0)$$

and

$$v = u_L \sin (L-L_0) + u_B \cos (L-L_0) \quad (4.4)$$

The variables z_k , u_k and v_k are thus calculated for $k = 1, \dots, 5$.

The equation of state for dry air is $p = \rho RT$ where ρ is the density $R = 287 \text{ J/K kg}$ is the gas constant for dry air and T is the temperature. In large scale atmospheric flows, the vertical pressure distribution may be assumed to follow the hydrostatic equation $\rho g z_p = -1$ where $g = 9.8 \text{ m/s}^2$. By applying the equation of state, an equation for temperature is achieved; $T = -p g z_p / R$, which may be discretized:

$$T_{k+1/2} = \frac{g}{R} \cdot \frac{z_k - z_{k+1}}{\ln\left(\frac{p_{k+1}}{p_k}\right)}; \quad k = 1, \dots, 4. \quad (4.5)$$

At integer levels, T is computed by linear interpolation with respect to the logarithm of pressure:

$$T_k = [\ln(p_{k-1/2}/p_k) \cdot T_{k+1/2} + \ln(p_k/p_{k+1/2}) \cdot T_{k-1/2}] / \ln(p_{k-1/2}/p_{k+1/2})$$

$$; k = 2, 3, 4 \quad (4.6)$$

Above 400 hPa the temperature is assumed to vary linearly with pressure:

$$T_k = T_{3/2} + \frac{T_{3/2} - T_2}{p_{3/2} - p_2} \cdot (p_k - p_{3/2}); \quad k = 1/2, 1 \quad (4.7)$$

The estimation of T at 1000 hPa is more complicated. Firstly, the horizontally averaged T at 850 and 925 hPa is computed:

$$\bar{T}_k = \frac{1}{I \cdot J} \cdot \sum_{i=1}^I \sum_{j=1}^J T_{i,j,k}; \quad k = 4, 9/2. \quad (4.8)$$

Secondly, it is assumed that the vertical gradient in \bar{T} between 925 and 1000 hPa is

$$\bar{T}_p = [T_p]_{AD} + \delta \quad (4.9)$$

where $[T_p]_{AD}$ is the dry adiabatic gradient and δ is the supposed deviation from it. Here, we have estimated

$$[T_p]_{AD} = \left[\left(\frac{p_5}{p_{9/2}} \right)^{R/c_p - 1} T_{9/2} / (p_5 - p_{9/2}) \right]$$

The deviation δ is put equal to the deviation from the dry adiabatic gradient between 925 and 850 hPa plus $3 \cdot 10^{-2}$ K/hPa. Having estimated \bar{T}_p , the averaged temperature at level $k = 5$ is

$$\bar{T}_5 = \bar{T}_{9/2} + \bar{T}_p \cdot (p_5 - p_{9/2})$$

To determine the temperature in actual grid points, the deviation from \bar{T} at each level is assumed to vary linearly with the logarithm to p:

$$T_5 = \bar{T}_5 + [(T_{9/2} - \bar{T}_{9/2}) \cdot \ln(p_4/p_5) + (T_4 - T_{9/2}) \cdot \ln(p_5/p_{9/2})] / \ln(p_4/p_{9/2}) \quad (4.10)$$

In order to compute the potential temperature θ , one could use the well known definition $\theta = T(p_5/p_k)^{R/c_p}$ directly. In practice, however, the calculation of T_k does not guarantee a stable atmosphere, and then θ is not a singlevalued function of pressure. Therefore, the stability parameter S is chosen, as defined by

$$S = \frac{R}{p^2} \left[\frac{R}{c_p} T - \frac{\partial T}{\partial(\ln p)} \right] \quad (4.11)$$

To compute θ , the more known formula $S = -e_p/\rho\theta$ is integrated. By definition the Exner function Π is:

$$\Pi = c_p (p/p_r)^{R/c_p} \quad (4.12)$$

where $p_r = 1000$ hPa. Since $c_p T = \theta \Pi$, one may write

$$\theta_p = -\frac{c_p}{R} p S / \Pi \quad (4.13)$$

The stability of the atmosphere may be controlled by the parameter S. This must be done in order to conserve the mean temperature of the atmosphere.

The procedure runs as follows. The stability parameter is computed

$$S_{k+1/2} = \frac{R}{2} \cdot \left[\frac{R}{c_p} \cdot T_{k+1/2} - \frac{T_{k+1} - T_k}{\ln(p_{k+1}/p_k)} \right] ; k = 1, 2, 3, 4$$

and (4.14)

$$S_{1/2} = \frac{R^2}{c_p p_{1/2}^2} T_{1/2}$$

where the temperature is assumed constant above 300 hPa. The estimated stability is corrected by

$$\hat{S}_k = \max \{S_k, S_{\min, k}\} \quad (4.15)$$

where S_{\min} is given by Table 4.1. Having computed \hat{S}_k , preliminary estimates of the potential temperature is given by

$$\theta_k^* = \theta_{k+1}^* + \frac{c_p}{R} \cdot \frac{p_{k+1/2}}{\pi_{k+1/2}} \hat{S}_{k+1/2} \cdot (p_k - p_{k+1}); \quad k = 1, 2, 3, 4$$

and (4.16)

$$\theta_5^* = T_5$$

Table 4.1: The minimum permitted value of the stability parameter S

k	P(hPa)	$S_{\min} (10^{-6} \text{ m}^4 \text{ s}^2 \text{ kg}^{-2})$
1/2	200	3.0
1 1/2	400	2.0
2 1/2	600	1.2
3 1/2	775	0.8
4 1/2	925	0.5

The final estimate of the potential temperature is

$$\theta_k = \theta_k^* + c_p \Delta T_{\text{adj}} / \pi_k \quad ; k = 1, 2, 3, 4, 5 \quad (4.17)$$

The corrective adjustment ΔT_{adj} is determined by requiring the mean temperature of the atmosphere to be conserved;

$$\Delta T_{\text{adj}} = - \frac{1}{p_5 - p_{1/2}} \sum_{k=1}^4 (\theta_k^* \pi_k^{-c_p T_k}) (p_{k+1/2} - p_{k-1/2}) / c_p, \quad (4.18)$$

and the potential temperature at integer levels are thus defined.

The next parameter to determine is z_e . The hydrostatic equation in e -coordinates may be written

$$z_e = - \frac{\theta}{g} \Pi_e. \quad (4.19)$$

For $k = 1, 2, 3$ and 4 is approximated:

$$(\Pi_e)_{k+1/2} = (\Pi_k - \Pi_{k+1}) / (\theta_k - \theta_{k+1}). \quad (4.20)$$

At 200 hPa ($k=1/2$) a relation between Π_e and the stability parameter S is utilized

$$(\Pi_e)_{1/2} = - (R\Pi_{1/2}/p_{1/2} \cdot c_p)^2 / S_{1/2} \quad (4.21)$$

The potential temperature at half-integer levels is now determined by

$$\theta_{k-1/2} = \theta_k + (\Pi_{k-1/2} - \Pi_k) / (\Pi_e)_{k-1/2} \quad ; k = 1, \dots, 5 \quad (4.22)$$

and finally,

$$(z_e)_k = - \theta_k \cdot (\Pi_e)_k / g; \quad k = 1/2, \dots, 9/2 \quad (4.23)$$

4.2 THE SURFACE FUNCTIONS

The input fields in pressure surfaces only implicitly take into account the ground surface topography, and that the lowermost pressure surfaces may be nonexistent in mountainous regions. The surfaces are supposed to be simply connected, and the wind and massfields includes the effects of the topography and the planetary boundary layer. Similarly, the dispersion model does not directly take the topography into account. However, it is taken into consideration through the meteorological fields. This approximation is justified by the fact that the major part of the sulphur emissions are found at low levels above the sea. The terrain height is thus put to zero.

In the following section, the fields at 1000 hPa are taken to be valid at the transition between the surface layer and the planetary boundary layer. In computing C_H , information about ground surface properties such as temperature T_G , roughness z_0 and boundary layer

height z_m is necessary. In Table 4.2 these properties are given for different ground surface types. The simplified method for the determination of ground surface temperature, may be generalized over land and sea-ice by introducing a diagnostic equation. However, several heuristic approaches must be made. To introduce an equation for sea surface temperature would require a complex air/sea-interaction model. Climatological values have been used instead (Pickard, 1970). The height of the surface layer is assumed to be

$$H_s = 0.04 \cdot z_m \quad (4.24)$$

Table 4.2: Ground surface properties

Surface type	z_0 (m)	z_m (min)(m)	z_m (max)(m)	T_G /surface layer stability
Open sea	10^{-3}	400	1000	T_G taken from seasonal maps
Icecov. sea	10^{-3}	400	650	$T_G \leq -1^{\circ}\text{C}/\text{isoterm}$
Open, snowcov. land	10^{-3}	400	650	$T_G \leq 0^{\circ}\text{C}/\text{isoterm}$
Mount./forrest sn.cov.land	$5 \cdot 10^{-2}$	550	850	$T_G \leq 2^{\circ}\text{C}/$ Halfway between neutral and isoterm
Open bare land	$5 \cdot 10^{-3}$	700	1000	Neutral stability
Mount./forrest bare land	10^{-1}	700	1000	Neutral stability

The local mixing height z_m over open sea is set to $z_m = z_m(\text{max})$ when $T_s - T_G \leq - (40\text{m}) \cdot g/c_p$. Otherwise over land, icecovered sea or open sea with $T_s - T_G > - (40\text{m}) \cdot g/c_p$:

$$z_m = \begin{cases} z_m(\text{max}) & ; Ri \leq 0 \\ z_m(\text{max}) - [z_m(\text{max}) - z_m(\text{min})] Ri/Ri_0 & ; 0 < Ri \leq Ri_0 \\ z_m(\text{min}) & ; Ri > Ri_0 \end{cases} \quad (4.25)$$

where $Ri = S_{9/2} / \left[\frac{|\vec{v}_5 - \vec{v}_4|}{p_5 - p_4} \right]^2$, $Ri_0 = 10$ and $S_{9/2}$ is determined from Eq. (4.14) (uncorrected value).

The bulk diffusion coefficient C_H may be computed by the Louis (1979) - formulae, which are explicit versions of the Businger, universal functions (Businger et al., 1971). These lead to

$$C_H = a^2 F_H \quad (4.26)$$

where

$$F_H = \frac{1}{0.74} \cdot \begin{cases} 1-2b Ri_B / (1-c |Ri_B|^{1/2}) & ; Ri_B \leq 0 \\ (1+b Ri_B)^{-2} & ; Ri_B > 0 \end{cases}$$

The surface layer bulk Richardson number is

$$Ri_B = gH_S (e_5 - e_G) / [(e_5 + e_G) |\vec{v}_5|^2 / 2] \quad (4.27)$$

where the ground surface potential temperature is estimated to

$$e_G = T_G \cdot \left(\frac{p_5 + H_S/8}{p_5} \right)^{R/c_p} \quad (4.28)$$

where H_S is given in metres. Further, $a = 0.35/\ln(H_S/z_0)$, $b = 4.7$ and $c = 5.3a^2 b (H_S/z_0)^{1/2}$.

The potential temperature e_s at the top of the surface layer, is estimated to

$$e_s = e_5 + (\Pi_s - \Pi_5) / (\Pi_e)_9/2 \quad (4.29)$$

where the corresponding Exner function is

$$\Pi_s = (z_4 \Pi_5 - z_5 \Pi_4) / (z_4 - z_5) \quad (4.30)$$

4.3 DIABATIC HEATING AND PRECIPITATION

So far we have enough information to estimate the value of a variable given in pressure surfaces at any isentropic surface with $e \in [e_{1/2}, e_5]$. There are, however, two very important variables left to be determined: the heating \dot{e} and the flux density of precipitation P . The heating function include three physical processes:

$$\dot{\epsilon} = \dot{\epsilon}_{\text{diff}} + \dot{\epsilon}_{\text{lat}} + \dot{\epsilon}_{\text{rad}} \quad (4.31)$$

where $\dot{\epsilon}_{\text{diff}}$ is turbulent heat conduction in the boundary layer, $\dot{\epsilon}_{\text{lat}}$ is the release of latent heat due to condensation and $\dot{\epsilon}_{\text{rad}}$ is heating due to terrestrial, infrared radiation. The direct absorption of heat due to solar radiation is omitted, the main effect being included in the term $\dot{\epsilon}_{\text{diff}}$ as the sun heats the ground. The precipitation may be of three types also:

$$P = P_{\text{fog}} + P_{\text{strat}} + P_{\text{conv}} \quad (4.32)$$

where P_{fog} is fog generation near the ground, P_{strat} is precipitation from stratiform clouds created by large scale condensation, and P_{conv} is convective precipitation. The released latent heat $\dot{\epsilon}_{\text{lat}}$ is also separated in accordance with (4.32).

4.3.1 Boundary layer processes

These processes include $\dot{\epsilon}_{\text{diff}}$ and P_{fog} . The eddy diffusion of potential temperature may be written

$$\dot{\epsilon}_{\text{diff}} = - F_p^{(\theta)} \quad (4.33)$$

where $F^{(\theta)}$ is the eddy flux density of θ through a constant pressure surface. It is positive when directed downwards (increasing p). Within the surface layer,

$$F^{(\theta)} = \rho g C_H |\vec{v}| (\theta - \theta_G) \quad (4.34)$$

and above the surface layer

$$F^{(\theta)} = - g K \theta_p \quad (4.35)$$

where K is the turbulent exchange coefficient in p -coordinates. Once again the approximations (2.22) are used to estimate K , but since the vertical coordinate is pressure, (3.29) cannot be used. However, the same technique is used, and hence for $k = 1, 2, 3, 4$:

$$(K_{\max})_{k+1/2} = \frac{1}{g \cdot \Delta t_{\text{adj}}} \frac{(p_{k+1} - p_k)(p_{k+3/2} - p_{k+1/2})(p_{k+1/2} - p_{k-1/2})}{p_{k+3/2} - p_{k-1/2}} \quad (4.36)$$

where by convention $p_{10/2} \equiv p_5$ and Δt_{adj} is a supposed adjustment time, $\Delta t_{\text{adj}} = 1800\text{s}$. The critical Richardson number has been given the value $Ri_c = 1/2$, and the Richardson number is for $k = 1, 2, 3, 4$:

$$Ri_{k+1/2} = S_{k+1/2} / \left(\frac{|\vec{v}_{k+1} - \vec{v}_k|}{p_{k+1} - p_k} \right)^2 \quad (4.37)$$

where $S_{k+1/2}$ is the uncorrected stability parameter (4.14). Finally it is supposed that $K_{1/2} = 0$. Consequently it is now assumed that

$$(\dot{e}_{\text{diff}})_k = \begin{cases} \frac{g K_{3/2}}{(p_{3/2} - p_{1/2})} \cdot \frac{\theta_2 - \theta_1}{p_2 - p_1} & ; k=1 \\ \frac{g}{p_{k+1/2} - p_{k-1/2}} \cdot [K_{k-1/2} \frac{\theta_{k-1} - \theta_k}{p_k - p_{k-1}} - K_{k+1/2} \frac{\theta_k - \theta_{k+1}}{p_{k+1} - p_k}] & ; k=2,3,4 \\ \frac{g}{p_5 - p_{9/2}} \cdot [K_{9/2} \frac{\theta_4 - \theta_5}{p_5 - p_4} - \rho_0 C_H |\vec{v}_5| (\theta_5 - \theta_G)] & ; k=5 \end{cases} \quad (4.38)$$

where $\rho_0 = 1.2923 \text{ kg m}^{-3}$ is the assumed air surface density. The estimated value of \dot{e}_{diff} is never permitted to exceed 1 K.day^{-1} in absolute value. In practice, however, the turbulent heat conduction is rarely different from zero for $k < 4$. It has in general significant non-zero values for $k = 5$.

The parameterization of fog is only active as long as the surface layer is stable, i.e. $\Delta P_{\text{fog}} = 0$ and $\dot{e}_{\text{lat}}^{\text{fog}} = 0$ unless

$$\theta_5 - \theta_G > 0. \quad (4.39)$$

It is assumed that the ground surface is wet, and hence the ground surface specific humidity equals the saturation specific humidity:

$$q_G = q_{\text{sat}}(T_G, p_5) \quad (4.40)$$

This may overestimate the fog generation in dry areas on the earth. The specific humidity in the lowermost part of the atmosphere is taken as

$$q_5 = Rh_5 \cdot q_{\text{sat}}(T_5, p_5) \quad (4.41)$$

Then, in order to create fog, it is required that

$$q_5 - q_G > 0 \quad (4.42)$$

If this is the case, then fog is assumed to be generated on the time-scale of $\Delta t_{\text{fog}} = 6$ h. The rate of generation of liquid water may approximately be written

$$q_w = \frac{1}{\Delta t_{\text{fog}}} \cdot (q_5 - q_G) / \left(1 + \frac{\epsilon L^2 q_G}{c_p R T_G^2}\right) \quad (4.43)$$

where the Clausius-Clapeyron equation has been integrated from the state (q_5, T_5) to the state $(q_5 - q_w \cdot \Delta t_{\text{fog}}, T_5 + \Delta T)$. The latent heat of condensation of water vapor is $L = 2.5 \cdot 10^6$ J/kg and the ratio between the gas-constants for dry air and water vapor is $\epsilon = 0.622$. The fog generation is assumed to be evenly distributed between 925 and 1000 hPa. Thus

$$P_{\text{fog}} = \begin{cases} \bar{q}_w \cdot \Delta p_{\text{fog}} / g & ; \text{ when } q_5 > q_G \text{ and } e_5 > e_G \\ 0 & ; \text{ all other cases} \end{cases} \quad (4.44)$$

where $\Delta p_{\text{fog}} = 75$ hPa. The released latent heat is

$$\dot{e}_{\text{lat}}^{\text{fog}} = L \cdot q_w \cdot \Delta p_{\text{fog}} / \Pi_5 \quad (4.45)$$

The values of P_{fog} and $\dot{e}_{\text{lat}}^{\text{fog}}$ is ascribed to the 1000 hPa-level ($k=5$) and their maximum values are adjusted so that $\dot{e}_{\text{lat}}^{\text{fog}} \leq 1\text{K} \cdot \text{day}^{-1}$ always.

The saturation specific humidity for water vapor over a flat water surface is

$$q_{\text{sat}}(T,p) = \epsilon \cdot e_{\text{sat}}(T)/p \quad (4.46)$$

where $e_{\text{sat}}(T)$ is partial pressure of water vapor over a plane water surface at saturation, which is tabulated in Smithsonian Meteorological Tables (1966), tables 94 and 96.

4.3.2 Convective precipitation

The conditions producing convective precipitation are an unstable boundary layer where the turbulent heat flux density is directed upwards, a conditionally stable atmosphere aloft, and a net convergence of humidity into the region of conditional instability. The present model is based upon the parameterization scheme originally proposed by Kuo (1965) and developed further by himself (Kuo, 1974) and Anthes (1977). All cumuli clouds are supposed to have their base at $p_{\text{bas}} = 925$ hPa. In order to judge the conditional stability aloft, the moist adiabat starting from 850 hPa is estimated by the formula.

$$T_c(p-\Delta p) = T_c(p) - (T_c)_p \cdot \Delta p (1+\Delta p/2p) \quad (4.47)$$

where T_c is the temperature at the adiabat, and its gradient is

$$(T_c)_p = \frac{RT_c}{c_p p} \cdot \left(1 + \frac{\epsilon L}{c_p T_c}\right) / \left(1 + \frac{\epsilon L}{c_p T_c} \cdot \frac{Lq_{\text{sat}}(T_c, p)}{RT_c}\right) \quad 4.48$$

Consequently:

$$(T_c)_4 = T_4$$

and for $k = 1, 2, 3$, $(T_c)_k$ is computed by using (4.47) and $\Delta p = p_{k+1} - p_k$. The top of the cumuli is supposed to exist at

$$p_{\text{top}} = p_{k+1/2} \quad (4.49)$$

where level no. k is the lowest level where

$$(T_c)_k < T_k \quad (4.50)$$

If (4.50) is not fulfilled for any $k = 1, 2, 3$, then $p_{\text{top}} = p_{1/2}$. The lowermost layer in the cloud is represented by the level $k_{\text{bas}} = 4$ and the uppermost by the level $k_{\text{top}} = k+1$ so that $p_{\text{top}} = p_{k+1/2}$, see Figure 4.3. The conditions for initiation of cumulus generation are that

$$Ri_{9/2} < 0.05 \text{ and } k_{\text{top}} < k_{\text{bas}} \quad (4.51)$$

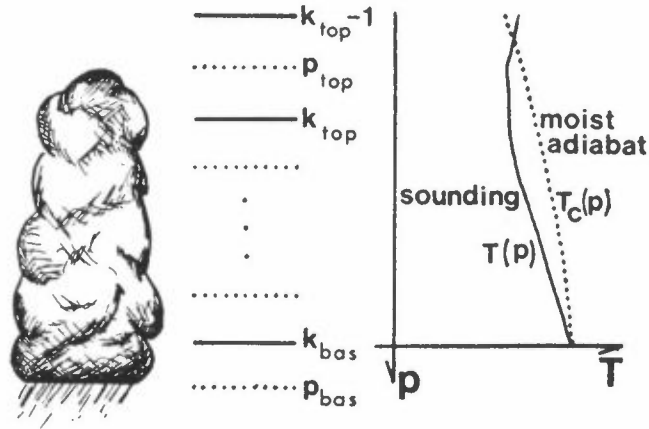


Figure 4.3: The definition of base and top of a model cumulus cloud.

If this is fulfilled, then the net convergence of specific humidity into the potential cloud region is computed according to Krishnamurti et al., (1976):

$$M_t = (Kq_p)_{\text{bas}} - (Kq_p)_{\text{top}} - \frac{1}{g} \int_{p_{\text{top}}}^{p_{\text{bas}}} qm^2 \nabla \cdot \frac{\vec{v}}{m} \delta p \quad (4.52)$$

where the exchange coefficient K is given by (2.22) and (4.36) and m is the map factor (2.9). In discretized form

$$M_t = K_{9/2} \frac{q_5 - q_4}{p_5 - p_4} + K_{k_{\text{top}}-1/2} \frac{q_{k_{\text{top}}-1} - q_{k_{\text{top}}}}{p_{k_{\text{top}}} - p_{k_{\text{top}}-1}} - \frac{1}{g} \sum_{k=k_{\text{top}}}^{k_{\text{bas}}} q_k (m^2 \nabla \cdot \frac{\vec{v}_k}{m}) (p_{k+1/2} - p_{k-1/2}) \quad (4.53)$$

Even if this influx of water vapor into the cloud region does not include pure advection, it is not correct physically to assume that all this water vapor contributes to cloud water. Some of it will normally also contribute to a general increase of the water vapor content. This was noted by Anthes (1977).

The main problem with (4.53) is that it includes the total turbulent transport of water vapor from the boundary layer. If all this water vapor is transformed into cloud water, an unphysical decrease of the relative humidity in the boundary layer would be the result. Therefore, the contribution to the generation of cloud water from the boundary layer, is only the amount which exceeds what is necessary to keep the relative humidity in the boundary layer unchanged. The flux density needed to keep the relative humidity unchanged, is

$$F^{(q)} = c_p K(T_p - RT/p c_p) / L \quad (4.54)$$

Now define

$$\Delta F^{(q)} = \max \left\{ K_{9/2} \left[\frac{q_5 - q_4}{p_5 - p_4} - \frac{c_p}{L} \left(\frac{T_5 - T_4}{p_5 - p_4} - \frac{RT_{9/2}}{c_p p_{9/2}} \right) \right]; 0 \right\} \quad (4.55)$$

The netto convergence of humidity into the cloud region, \tilde{M}_t , which contribute to the generation of cloud water, is given by (4.53) with the term $K_{9/2} (q_5 - q_4) / (p_5 - p_4)$ replaced by $\Delta F^{(q)}$. If \tilde{M}_t as computed in in this manner is less than zero, there is no humidity to produce cloud water. In that case, $\tilde{M}_t = 0$.

The total support of humidity needed to produce a cloud which fills up the whole grid volume between p_{bas} and p_{top} is

$$C = \frac{1}{g} \int_{p_{top}}^{p_{bas}} [q_{sat}(T_c, p) - q + \frac{c_p}{L} (T_c - T)] \delta p, \quad (4.56)$$

or discretized;

$$C = \frac{1}{g} \sum_{k=k_{\text{top}}}^{k_{\text{bas}}} [q_{\text{sat}}((T_C)_k, p_k) - q_k + \frac{c_p}{L} ((T_C)_k - T_k)] (p_{k+1/2} - p_{k-1/2}). \quad (4.57)$$

The flux density of precipitation released in layer no. k is now for $k = k_{\text{top}}$ to $k = k_{\text{bas}}$,

$$(\Delta P_{\text{conv}})_k = \frac{\tilde{M}_t}{C} \cdot \frac{c_p}{g \cdot L} [(T_C)_k - T_k] \cdot (p_{k+1/2} - p_{k-1/2}) \quad (4.58)$$

and the released latent heat:

$$(\dot{e}_{\text{lat}}^{\text{conv}})_k = \frac{\tilde{M}_t}{C} \cdot \frac{c_p}{\Pi_k} \cdot [(T_C)_k - T_k]. \quad (4.59)$$

The released precipitation is never permitted to exceed a value corresponding to a released latent heat of $\dot{e} = 1 \text{ Kh}^{-1}$.

4.3.3 Stratiform precipitation

Large scale precipitation is released by frontal circulations and orographic lifting. The information of such flows is presumed to be contained in the analysed wind field. This kind of precipitation is called stratiform precipitation, since it may be present in an absolutely stable atmosphere. It is not supposed to exist simultaneously with convective precipitation. If the conditions (4.51) are fulfilled, then the lowest layer of possible stratiform precipitation is $k = k_{\text{top}} - 1$. Otherwise, all layers may be involved.

Even if the given relative humidity is smaller than one in a given grid point, stratiform precipitation may exist (Sundqvist, 1981). The stratiform cloudiness in a layer k is for $k = 1, 2, 3, 4$ or 5 ,

$$a_k = \left(\max \left\{ \frac{Rh_k - Rh_{c,k}}{1 - Rh_{c,k}}, 0 \right\} \right)^2 \quad (4.60)$$

Table 4.3: The critical relative humidity, Rh_c

k	p(hPa)	Rh_c
1	300	0.80
2	500	0.80
3	700	0.80
4	850	0.80
5	1000	0.92

where the critical humidity Rh_c is given in Table 4.3. In addition to have a non-zero cloudiness, the release of precipitation is also conditioned by rising air, i.e. air parcels must experience a decreasing pressure. The individual rate of change of pressure, ω , is the vertical atmospheric velocity when pressure is vertical coordinate. The equation of continuity in pressure coordinates is

$$\omega_p = -m^2 \nabla \cdot \frac{\vec{v}}{m}. \quad (4.61)$$

This equation may be integrated with respect to pressure. Assuming $\omega_{1/2} = 0$ ($p_{1/2} = 200$ hPa), the discretized form leads to

$$\omega_{k+1/2} = \sum_{l=1}^k (-m^2 \nabla \cdot \frac{\vec{v}_l}{m}) (p_{l+1/2} - p_{l-1/2}) \quad (4.62)$$

for $k = 1, 2, 3, 4$. To estimate ω at integer levels, a second order interpolation scheme with respect to pressure is employed. Knowing ω at three values of p : $\omega_A = \omega(p_A)$, $\omega_B = \omega(p_B)$ and $\omega_C = \omega(p_C)$, the value of ω at any value of p may be estimated by

$$\omega(p) = \omega_B + [\alpha \cdot (p - p_A) + \beta] (p - p_B)$$

where

$$\alpha = \frac{(p_A - p_C)(\omega_A - \omega_B) - (p_A - p_B)(\omega_A - \omega_C)}{(p_A - p_B)(p_A - p_C)(p_B - p_C)} \quad (4.63)$$

and

$$\beta = \frac{\omega_A - \omega_B}{p_A - p_B}$$

Using this formulae, ω_k is estimated for $k = 1, 2, 3, 4$ and 5 . Now define for $k = 1, 2, 3, 4$ and 5

$$\delta_k = \begin{cases} 1 & \text{for } \omega_k < 0 \\ 0 & \text{for } \omega_k \geq 0 \end{cases} \quad (4.64)$$

Stratiform precipitation is present provided that $\delta_k = 1$ and $a_k > 0$. In that case, the production of liquid water is

$$\left(\frac{dq_w}{dt}\right)_k = -\delta_k \cdot a_k \cdot \left(\frac{dq_{sat}}{dt}\right)_k \quad (4.65)$$

By utilizing the Clausius-Clapeyron equation and the first law of thermodynamics, an expression for dq_{sat}/dt is deduced,

$$\left(\frac{dq_{sat}}{dt}\right)_k = \frac{RT_k}{p_k} \cdot \omega_k \cdot q_{sat}(T_k, p_k) \cdot (\epsilon L - c_p T_k) / (c_p RT_k^2 + \epsilon L^2 q_{sat}(T_k, p_k)) \quad (4.66)$$

Having initiated stratiform precipitation in the layer k with pressure thickness $p_{k+1/2} - p_{k-1/2}$, the thickness of the total precipitating layer is determined by the moist stability aloft. The moist adiabat starting in the layer k is computed from (4.47) with $(T_c)_k = T_k$. The base of the stratiform cloud is $p_{bas} = p_{k+1/2}$ and the top is $p_{top} = p_{\iota+1/2}$ where layer no. ι is the lowest layer where $(T_c)_\iota < T_\iota$. Once again $k_{bas} = k$ and $k_{top} = \iota + 1$. The lowest permitted value of k_{top} is $1/2$. If $k_{top} = k_{bas}$ then $p_{bas} = p_{k+1/2}$, and the stratiform cloud covers only one model layer.

The contribution to the precipitation flux density is now estimated to

$$(\Delta P_{strat})_k = \frac{p_{k+1/2} - p_{k-1/2}}{p_{bas} - p_{top}} \cdot \sum_{\iota=k_{top}}^{k_{bas}} \left(\frac{dq_w}{dt}\right)_\iota (p_{\iota+1/2} - p_{\iota-1/2}) / g, \quad (4.67)$$

and the released latent heat is

$$(e_{lat}^{strat})_k = \frac{L}{\pi_k (p_{bas} - p_{top})} \sum_{\iota=k_{top}}^{k_{bas}} \left(\frac{dq_w}{dt}\right)_\iota (p_{\iota+1/2} - p_{\iota-1/2}). \quad (4.68)$$

In summarizing the effects of condensation and precipitation, the total flux density of precipitated water through a level k is given by

$$P_k = \sum_{i=1}^k [(\Delta P_{\text{conv}})_i + (\Delta P_{\text{strat}})_i] + (P_{\text{fog}})_k \quad (4.69)$$

where $(P_{\text{fog}})_k = 0$ for $k = 1, 2, 3, 4$ and given by Eq. (4.44) for $k = 5$. Similarly for the released latent heat

$$(\dot{e}_{\text{lat}})_k = (\dot{e}_{\text{lat}}^{\text{conv}})_k + (\dot{e}_{\text{lat}}^{\text{strat}})_k + (\dot{e}_{\text{lat}}^{\text{fog}})_k \quad (4.70)$$

where $(\dot{e}_{\text{lat}}^{\text{fog}})_k = 0$ for $k = 1, 2, 3, 4$ and given by Eq. (4.45) for $k = 5$.

4.3.4 Terrestrial radiation

A major part of the energy received from the sun, is electromagnetic radiation with wavelengths within a range that is not absorbed in the atmosphere (99% of the radiation is within $0.2 \mu\text{m}$ - $4 \mu\text{m}$). The corresponding energy emitted to the universe by radiation from the earth, has wavelengths within a range that may be effectively absorbed and re-emitted in the atmosphere. The mean black-body temperature of the earth is about 250 K, and 99% of the radiation is emitted within the range $5 \mu\text{m}$ - $100 \mu\text{m}$. The most important gas in the atmosphere having corresponding possible transitions between vibrational states in the molecules, is water vapor. The second important gas is CO_2 . Ozone also contributes within a narrow spectral band, however, the major contribution is in the stratosphere. On the other hand ozone and other gases which interact with terrestrial radiation, are created in the lower atmosphere by human activities. The effects of those are not taken into account here. Another very important, radiatively active constituent present in the atmosphere, is liquid water in clouds. Clouds of thickness about 100 m or more can be treated as black-body radiators.

The present method to compute radiative heating in the atmosphere, utilizes emissivity functions that include absorption functions integrated over all wavelengths (see e.g. Bodin, 1979). The heating of the atmosphere due to radiation as measured by \dot{e} , is

$$\dot{e}_{\text{rad}} = g\Phi_p/\pi \quad (4.71)$$

where Φ is the net energy flux density through horizontal surfaces due to radiation. The main problem is to determine Φ as a function of p . The contribution to Φ at pressure p of radiation emitted in a layer $\delta p'$ beyond the pressure value p' (see Figure 4.4) is

$$\begin{aligned} \delta\Phi(p) &= \sigma T(p')^4 \cdot [E(p, p'+\delta p') - E(p, p')] \\ &= \sigma T(p')^4 \cdot \frac{\partial E(p, p')}{\partial p'} \delta p' \end{aligned} \quad (4.72)$$

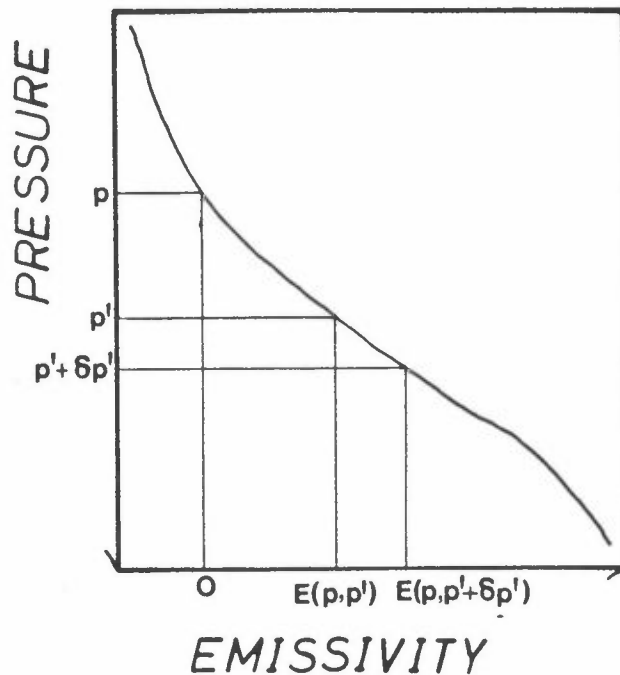


Figure 4.4: Contribution to radiation flux density at pressure level p from the layer between p' and $p' + \delta p'$.

Here $\sigma = 5.6697 \cdot 10^{-8} \text{ Wm}^{-2} \text{ K}^{-4}$ is the Stefan-Boltzman constant and $E(p, p')$ is the emissivity of the layer $p-p'$, which may be written

$$E(p, p') = \int_0^{\infty} \int_p^{p'} \pi \frac{B(\nu, p'')}{\sigma T(p'')^4} \cdot \frac{dA_{\nu}}{dp''} \delta p'' \delta \nu \quad (4.73)$$

Where ν is frequency, B is the Planck function for black-body radiation and A_{ν} is the fractional absorption at frequency ν . The emissivity of black bodies, such as clouds and the ground, is unity (1).

By integrating (4.72) the total $\Phi(p)$ is determined. Since $\delta p'$ is negative for $p' < p$ and positive for $p' > p$, the contribution from below, Φ^\uparrow , is separated from the contribution from aloft Φ^\downarrow . Thus,

$$\begin{aligned} \Phi(p) &= \Phi^\uparrow(p) - \Phi^\downarrow(p); \\ \Phi^\uparrow(p) &= \sigma \int_p^{p_s} T(p')^4 \frac{\partial E(p, p')}{\partial p'} \delta p' + [1 - E(p, p_s)] \sigma T_G^4 \\ \Phi^\downarrow(p) &= \sigma \int_p^0 T(p')^4 \cdot \frac{\partial E(p, p')}{\partial p'} \delta p' \end{aligned} \quad (4.74)$$

The extra term added to Φ^\uparrow is the contribution from the ground surface which is considered black.

In the present model clouds, water vapor and CO_2 are taken into account when estimating E . In practice, clouds are taken into account separately. To discretize (4.74), the vertical separation sketched in Figure 4.1 is extended upwards to $p = 0$, so that $p_0 = 100$ hPa and $p_{-1/2} = 0$. Also at the lowermost levels, the vertical separation differs from Figure 4.1. Thus $p_5 = 962.5$ hPa and $p_{11/2} = 1000$ hPa. The vertical structure specially designed for the radiation calculations are sketched in Figure 4.4. The fractional cloud cover is

$$a_m = \begin{cases} 0 & ; m = 0 \\ (\max\{\frac{Rh_m - Rh_{c,m}}{1 - Rh_{c,m}}, 0\})^2 & ; m = 1, 2, 3, 4 \\ (\max\{\frac{Rh_{m+1/2} - Rh_{c,m+1/2}}{1 - Rh_{c,m+1/2}}, 0\})^2 & ; m = 5 \end{cases} \quad (4.75)$$

However, no boundary layer clouds are permitted when it is unstable,

$$a_5 = 0 \text{ when } Ri_{11/2} \leq 0.05 \quad (4.76)$$

The effective radiation temperature at $p = 0$ is set to $T_{-1/2} = 140\text{K}$ in order to take into consideration radiation due to active gases very high up in the atmosphere. At $p = 100$ hPa, the temperature is estimated by a linear interpolation of the black-body flux density,

$$T_0^4 = (T_{-1/2}^4 + T_{1/2}^4)/2 \quad (4.77)$$

m	p(hPa)	
-1/2	0	---T, r
0	100	T, a, q, Δr
1/2	200	---T, r, φ
1	300	T, a, q, Δr, θ _{rad}
1 1/2	400	-----
2	500	-----
2 1/2	600	-----
3	700	-----
3 1/2	775	-----
4	850	-----
4 1/2	925	-----
5	962.5	-----
5 1/2	1000	-----

Figure 4.5: Special information surfaces only used when calculating terrestrial radiation.

The specific humidity at 100 hPa is zero, $q_0 = 0$. At 962.5 hPa, the needed variables are estimated by

$$q_5 = q_{11/2} \text{ and } T_5 = \frac{(\Pi_5 - \Pi_{9/2})T_{11/2} + (\Pi_{11/2} - \Pi_5)T_{9/2}}{\Pi_{11/2} - \Pi_{9/2}} \quad (4.78)$$

where Π_5 is the Exner function directly calculated from p_5 .

The discretized formulae for Φ^\uparrow and Φ^\downarrow are, when fractional cloud cover is taken into account; for $m = 0, 1, 2, 3, 4, 5$:

$$\begin{aligned} \Phi_{m+1/2}^{\downarrow} &= \sum_{\iota=0}^m \{ \sigma T_{\iota}^4 [E(p_{m+1/2}, p_{\iota-1/2}) - E(p_{m+1/2}, p_{\iota+1/2})] (1-a_{\iota}) \\ &\quad + \sigma T_{\iota+1/2}^4 [1-E(p_{m+1/2}, p_{\iota-1/2})] a_{\iota} \} \cdot \prod_{i=\iota+1}^m (1-a_i); \quad (4.79a) \end{aligned}$$

$$\begin{aligned} \Phi_{m+1/2}^{\uparrow} &= \sum_{\iota=m+1}^5 \{ \sigma T_{\iota}^4 [E(p_{m+1/2}, p_{\iota+1/2}) - E(p_{m+1/2}, p_{\iota-1/2})] (1-a_{\iota}) \\ &\quad + \sigma T_{\iota-1/2}^4 [1-E(p_{m+1/2}, p_{\iota-1/2})] a_{\iota} \} \cdot \prod_{i=m+1}^{\iota-1} (1-a_i). \quad (4.79b) \\ &\quad + \sigma T_{11/2}^4 [1-E(p_{m+1/2}, p_{11/2})] \prod_{i=m+1}^5 (1-a_i) \end{aligned}$$

The net flux density is for $m = 0, \dots, 5$:

$$\Phi_{m+1/2} = \Phi_{m+1/2}^{\uparrow} - \Phi_{m+1/2}^{\downarrow}. \quad (4.80)$$

In the interior of a black-body (e.g. a cloud), the net flux density will always vanish and there is no radiative heating. Due to discretization approximations, this will not be the result from Eqs. (4.79)-(4.80) for cloudy layers unless there are clouds at the layer above and clouds/ground surface at the layer underneath. Therefore the net flux density (4.80) cannot be applied directly. Define for $m = 1, 2, 3, 4, 5$ the coefficient

$$b_m = \max \{ 0, a_m - a_{m-1}, a_m - a_{m+1} \}, \quad (4.81)$$

where by convention $a_6 \equiv 1$ since the ground surface is black. This coefficient contains the part of a possible black body at level m which does not have a black body radiating towards it at both neighbour levels. The radiative heating is now for $m = 1, 2, 3, 4, 5$:

$$(\dot{e}_{\text{rad}})_m = (1-b_m) \cdot \frac{g}{\Pi_m} \frac{\Phi_{m+1/2} - \Phi_{m-1/2}}{p_{m+1/2} - p_{m-1/2}} \quad (4.82)$$

The value for $m = 5$ is taken to estimate the heating at 1000 hPa.

The emissivity function E takes into account water vapor (v) and CO_2 (c), that is

$$E(p, p') = E_V(p, p') + E_C(p, p') \quad (4.83)$$

An estimates of E_V has been given by Jacobs et al. (1974) as a function of the optical depth r between p and p' :

$$E_V(p, p') = \varepsilon_V(r(p, p')) \quad (4.84)$$

The optical depth is

$$r(p, p') = \left| \frac{1}{g} \int_p^{p'} (p''/p_R)^{1/2} \cdot q(p'') \delta p'' \right|, \quad (4.85)$$

where $p_R = 1000$ hPa.

The functions given by Jacobs et al. (1974) has been somewhat altered in order to have a continuous function,

$$\varepsilon_V(r) = \begin{cases} 0.024 \cdot \log_{10} r + 0.120 & ; \log_{10} r < -4 \\ 0.104 \cdot \log_{10} r + 0.440 & ; \log_{10} r \in [-4, -3> \\ 0.121 \cdot \log_{10} r + 0.491 & ; \log_{10} r \in [-3, -3/2> \\ 0.146 \cdot \log_{10} r + 0.527 & ; \log_{10} r \in [-3/2, -1> \\ 0.161 \cdot \log_{10} r + 0.542 & ; \log_{10} r \in [-1, 0> \\ 0.136 \cdot \log_{10} r + 0.542 & ; \log_{10} r \geq 0 \end{cases} \quad (4.86)$$

where r is given in CGS-units (i.e. g/cm^2 , $r_{\text{CGS}} = 0.1 r_{\text{SI}}$). Similarly, the emissivity for CO_2 is given by Kondratyev (1969) as a function of the optical depth c of CO_2 :

$$E_C(p, p') = \varepsilon_C(c(p, p')) \quad (4.87)$$

where

$$c(p, p') = 0.415 \cdot |p - p'|, \quad (4.88)$$

p is measured in units of hPa (= mb), and

$$\varepsilon_C(c) = 0.185 \cdot [1 - \exp(-0.392 \cdot c^{0.4})]. \quad (4.89)$$

Eq. (4.88) assumes a vertically uniform concentration of CO_2 of 320 ppm.

In the actual calculations performed, the optical thicknesses Δr and Δc are computed for $m = 0, 1, 2, 3, 4, 5$;

$$\Delta r_m = \left| \frac{1}{g} (p_m/p_{11/2})^{1/2} q_m (p_{m+1/2} - p_{m-1/2}) \right| \quad (4.90)$$

and

$$\Delta c_m = 0.415 \left| p_{m+1/2} - p_{m-1/2} \right|. \quad (4.91)$$

The optical depths counted from $p = 0$ are then given by

$$\Lambda_{r_{m+1/2}} = \sum_{\iota=0}^m \Delta r_{\iota} \quad \text{and} \quad \Lambda_{c_{m+1/2}} = \sum_{\iota=0}^m \Delta c_{\iota} \quad (4.92)$$

The optical thickness between arbitrary levels are then

$$r(p_k, p_m) = \left| \Lambda_{r_k} - \Lambda_{r_m} \right| \quad \text{and} \quad c(p_k, p_m) = \left| \Lambda_{c_k} - \Lambda_{c_m} \right| \quad (4.93)$$

which by (4.86) and (4.89) gives $E_v(p_k, p_m)$ and $E_c(p_k, p_m)$, and finally the total emissivity $E(p_k, p_m) = E_v + E_c$.

4.4 CHOICE OF ISENTROPIC SURFACES

As described in sections 4.1, 4.2 and 4.3, the relevant meteorological fields are calculated every twelve hours at levels as given in Figure 4.1. To calculate these fields at any intermediate time-level, a linear interpolation in time is performed:

$$h(t) = [(t - \tau_n)h(\tau_{n+1}) + (\tau_{n+1} - t)h(\tau_n)] / (\tau_{n+1} - \tau_n) \quad (4.94)$$

where τ_n signifies the synoptic time-level no n within the simulation period, h is any of the meteorological variables defined in Figure 4.1 and t is a time-level such that $\tau_n \leq t < \tau_{n+1}$.

The value of the geopotential height of an atmospheric level with potential temperature θ may now be determined. Firstly, the heights of the integer pressure surfaces are calculated:

$$z_5 = (z_\theta)_{9/2} \cdot (\theta_5 - \theta_s)$$

and for $k = 1, 2, 3, 4$: (4.95)

$$z_k = (z_\theta)_{k+1/2} (\theta_k - \theta_{k+1}).$$

If θ is smaller than the surface value θ_s , the geopotential height is indefinite since there is no level in the atmosphere in the actual grid point having the potential temperature θ . Suppose that $\theta \geq \theta_s + \varepsilon$ where $\varepsilon = 1K$, i.e. θ defines an ordinary point see eq. (3.1); or that θ defines the ground surface: $\theta = \theta_s$.

The geopotential height of the level with potential temperature θ is then

$$z(\theta) = \begin{cases} z_1 + (z_\theta)_{1/2}(\theta - \theta_1) & ; \theta \geq \theta_1 \\ z_{k+1} + (z_\theta)_{k+1/2}(\theta - \theta_{k+1}) & ; \theta_{k+1} \leq \theta < \theta_k \\ z_5 + (z_\theta)_{9/2}(\theta - \theta_5) & ; \theta_s + \varepsilon \leq \theta < \theta_4 \end{cases} \quad (4.96)$$

For the variables u , v and $\dot{\theta}$, here signified by h ;

$$h(\theta) = \begin{cases} h_1 & ; \theta > \theta_1 \\ [(\theta - \theta_{k+1}) h_k + (\theta_k - \theta) h_{k+1}] / (\theta_k - \theta_{k+1}) & ; \theta_{k+1} < \theta \leq \theta_k \\ h_5 & ; \theta_s + \varepsilon \leq \theta \leq \theta_5 \\ & \text{or } \theta = \theta_s \end{cases} \quad (4.97)$$

As mentioned in section (3.6), u and v have to be estimate also in extraordinary points ($\theta < \theta_s + \varepsilon$) in order to be able to calculate the horizontal transport,

$$(u, v)(\theta) = (u_5, v_5) \quad ; \quad \theta < \theta_s + \varepsilon. \quad (4.98)$$

The precipitation is

$$P(\theta) = \begin{cases} 0 & ; \theta > \theta_1 \\ [(\theta - \theta_{k+1})P_k + (\theta_k - \theta)P_{k+1}] / (\theta_k - \theta_{k+1}) & ; \theta_{k+1} < \theta \leq \theta_k \\ P_5 & ; \theta_{s+\varepsilon} < \theta \leq \theta_5 \text{ or } \theta = \theta_s, \end{cases} \quad (4.99)$$

and finally the stability

$$z_\theta(\theta) = \begin{cases} (z_\theta)_{1/2} & ; \theta > \theta_{1/2} \\ [(\theta - \theta_{k+1/2})(z_\theta)_{k-1/2} + (\theta_{k-1/2} - \theta)(z_\theta)_{k+1/2}] / (\theta_{k-1/2} - \theta_{k+1/2}) & ; \theta_{k+1/2} < \theta \leq \theta_{k-1/2} \\ (z_\theta)_{9/2} & ; \theta_{s+\varepsilon} < \theta \leq \theta_{9/2} \end{cases} \quad (4.100)$$

Isentropic surfaces in the atmosphere are always in motion. A surface that is defined by a certain value of potential temperature, may exist high in the atmosphere over an area during one period, but be nonexistent during another. There are in particular large seasonal variations. In an isentropic coordinate-surface model, it is therefore important to choose surfaces that describe the atmosphere with optimal resolution during the period of simulations. It is not advisable to keep the same isentropic surfaces for a longer period of time than a month. If one wishes to simulate a longer time period (e.g. a whole year), it is separated into suitable subperiods not longer than a month. The results of the simulations for one subperiode are carried over to the next by interpolation.

The maximum possible number of ordinary isentropic surfaces are L (see Figure 3.2), in addition to the ground surface. L should always be greater or equal to 3. In the present version of the model $L = 10$ but this is easy to change. In order to define the optimum isentropic surfaces, the computed potential temperature at the ground surface, $\theta_s(x,y)$ is used as basic information. Let $\theta_{\max}(\tau_n)$ and $\theta_{\min}(\tau_n)$ be the maximum and minimum value of $\theta_s(\tau_n)$ for the synoptic timelevel τ_n .

Now define

$$e_A = \max \{e_{\max}(\tau_n)\}_{n=1}^N$$

and

(4.101)

$$e_B = \max \{e_{\min}(\tau_n)\}_{n=1}^N$$

where N is the number of synoptic time-levels during the period. The isentropic surfaces are now defined so that there are at least two ordinary coordinate surfaces at any time and place, and that there always exists an area with the number of L ordinary surfaces. With e_A and e_B measured in kelvin (K), this is accomplished as follows. The lowermost surface is

$$e_L = \text{Int} \{e_B + \delta_1\} \quad (4.102)$$

where $\text{Int}\{x\}$ is the largest integer number $\leq x$ and $\delta_1 = 2.5$ K. For $i = 3, \dots, L-1$, the surfaces are

$$e_i = e_{i+1} + \Delta e \quad (4.103)$$

where

$$\Delta e = \text{Int} \{ (e_A - e_B + \delta_2) / (L-2) \} \quad (4.104)$$

and $\delta_2 = 1.5$ K. Further,

$$e_2 = \text{Int} \{e_A + \delta_2\} \quad (4.105)$$

and finally the uppermost surface is

$$e_1 = e_2 + \Delta e \quad (4.106)$$

Having defined the isentropic surfaces and methods to calculate the meteorological fields at these, the simulation of sulphur dispersion can be made from any initial state of concentration distribution. As output from the model, daily accumulated wet and dry deposition is given in addition to concentration fields at levels of constant

geopotential height. Knowing the concentrations c_{ι} at surfaces e_{ι} , $\iota = 1, \dots, M$ (where M is the lowermost ordinary level) and the concentration at the top of the surface layer c_s , the concentration may be estimated at a level z . At approximately the level of ground level air sampling ($z = 1\text{m}$), the concentration is calculated consistently with the dry deposition speed at 1m , v_{dG} , and the state of turbulence in the surface layer,

$$c(z=1\text{m}) = c_s \cdot C_{HS} |\vec{v}_s| / (C_H |\vec{v}_s| + v_{dG}). \quad (4.107)$$

Here, the top of the surface layer is taken to be at 40 m,

$$c(z=40\text{ m}) = c_s \quad (4.108)$$

If one wishes to compute the concentration at a level between 1 m and 40 m then the aerodynamic bulk, drag coefficient C_M must be estimated (e.g by use of the Louis (1983)-functions). Further, the wind speed $|\vec{v}(z)| = |\vec{v}_s| \cdot (C_{MS}/C_M(z))$ is calculated, and finally, $c(z) = c_s (1+v_{dG}/C_H(z)|\vec{v}(z)|) / (1+v_{dG}/C_H |\vec{v}_s|)$. This is, however, not computed in the present version of the model. At a level z above the surface layer, the concentration is

$$c(z) = \begin{cases} [c_{\iota+1}(z_{\iota}-z) + c_{\iota}(z-z_{\iota+1})] / (z_{\iota}-z_{\iota+1}); & z_{\iota+1} \leq z < z_{\iota} \\ & \text{and } \iota = 1, \dots, M \\ \max \{0, c_1(z_*-z) / (z_*-z_1)\} & ; z \geq z_1 \end{cases}$$

where $z_* = z_1 + 1000\text{ m}$, $z_{M+1} = 0\text{ m}$ and $c_{M+1} = c_s$. In the present version of the model, the concentrations are calculated at $z = 5000\text{ m}$, 4000 m , 3000 m , 2000 m , 1000 m , 40 m and 1 m .

5 PROGRAMME STRUCTURE

The total model consists of four programme packages which are run in sequence. This is shown in Figure 5.1. The present file names on NILUS ND-560 CX is given. The two first programmes (I and II) are suited to fit the data as filed on the tapes from NCAR. These therefore must be changed when data from other sources are used. Even though the comment-statements should give a reasonable description, the different parts of the programmes III and IV are summarized below.

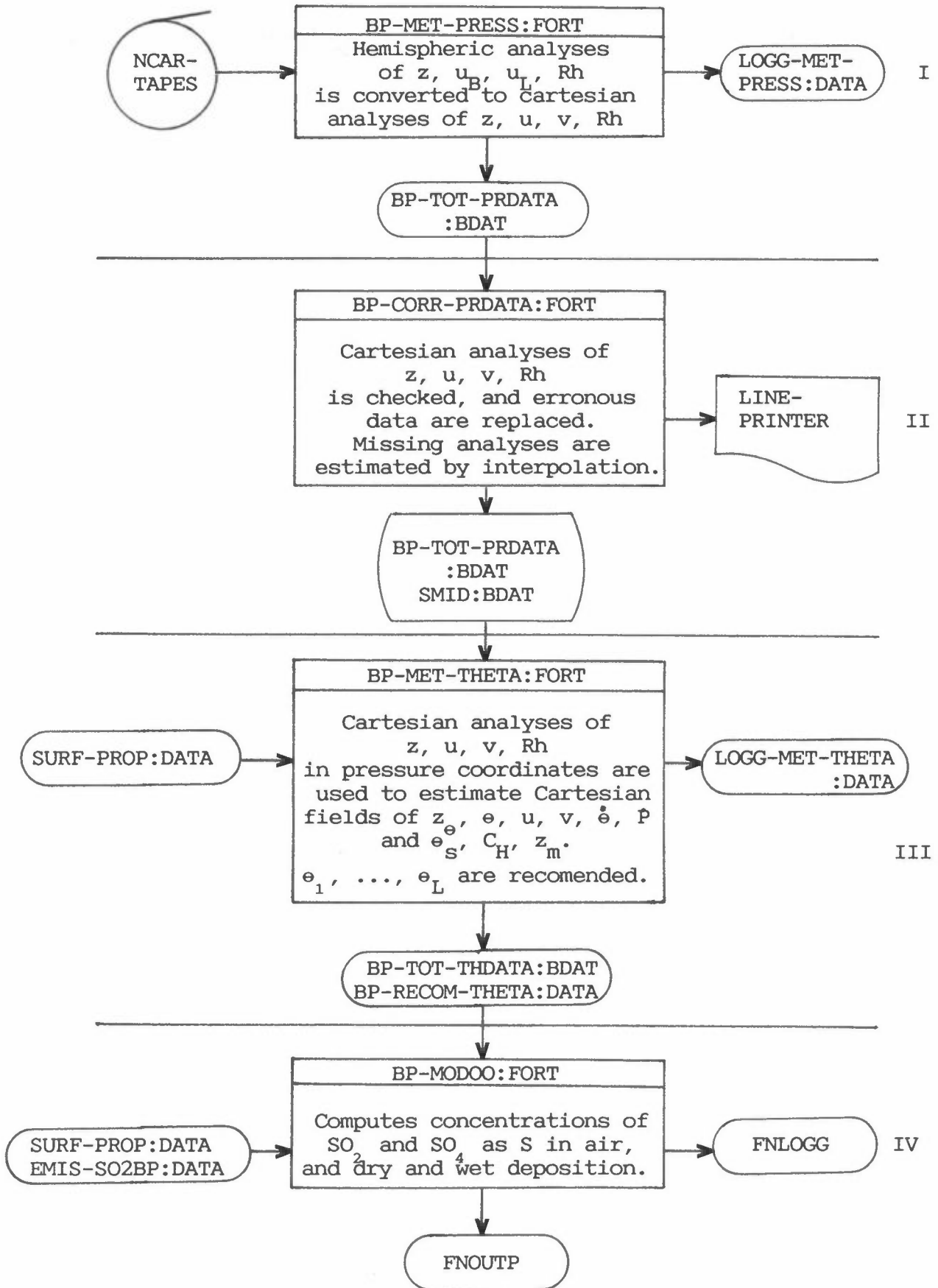


Figure 5.1: Sketch of the modelling procedure from meteorological analyses and processing through computed concentration.

III: BP-MET-THETA:FORT

METTH: Main programme; reads input, writes output, computes recommended values of e_1, \dots, e_L .

Calls routines: SURFPR, TEMP, THANA.

SURFPR: Subroutine; reads surface properties and stores in an array.

TEMP: Subroutine; computes temperature T , assures that the mean value of z at each level is kept constant i time.

THANA: Subroutine; computes $z_e, e, u, v, \dot{e}, P, e_s, C_H$ and z_M from $z, u, v, T, Rh. 12$;

IV: BP-MODOO:FORT

ARCTIC: Main programme; defines constants, controles stepping of synoptic time-intervals. Calls routines: HEADING, EMIS, SURF, METASS, EXTRA, RUN, OUTPUT.

OUTPUT: Subroutine; interpolates concentration fields to levels of constant geopotential height, z , and writes on file. The total wet and dry deposition of S since last call to OUTPUT or since the start of integration are written to file. Concentration at e -surfaces and deposition in six chosen gridpoints are written to the logg. Deposition arrays are reset to zero.

HEADING: Subroutine; writes a heading to the logg.

EMIS: Subroutine; reads emissions and stores in an array.

SURF: Subroutine; reads surface properties and stores in an array.

- METASS: Subroutine; reads input of meteorological fields: z_{θ} , θ , u , v , $\dot{\theta}$, P , e_s , C_H and z_M , and arranges so that the value of any of the functions may be computed in between synoptic hours by linear interpolation.
- RUN: Subroutine; controls the integration in between synoptic hours. Calculate the date and time for the present concentration-fields. Calls routines: WIND, SMOLAR, PHYS, EXTRA, SECT.
- SECT: Subroutine; estimates fictitious subterrain values of the concentrations.
- WIND: Subroutine; computes the wind in isentropic surfaces from analyses in isobaric. Fictitious, subterrain values are estimated to the value on top of the surface layer.
- EXTRA: Subroutine; computes for each gridpoint the level no. $l=M$ of the lowermost isentropic surface that is ordinary.
- PHYS: Subroutine; calculates the contributions to the concentration changes from emissions, vertical transport relative to the isentropic surfaces, vertical diffusion, dry deposition, and precipitation scavenging.
- SMOLAR: Subroutine; calculates the contributions to the concentration changes from horizontal transport in isentropic surfaces.

6 ACKNOWLEDGEMENT

The author is indepted to Dr. Brynjulf Ottar for having had the opportunity to apply ideas and theories in developing the present model.

7 REFERENCES


- AGASP (1984) Geophys. Res. Lett., 11 (5), 359-472, (spesial issue).
- Anthes, R.A., (1977) A cumulus parameterization scheme utilizing an one dimensional cloud model. Mon. Wea. Rev., 105, 270-286.
- Arctic Air Chemistry, (1985) Atmos. Environ., 19, (12), 1987-2208, (special issue).
- Barrie, L.A. (1981) The prediction of rain acidity and SO₂ scavenging in eastern North America. Atmos. Environ., 15, 31-41.
- Businger, J.A., Wyngaard, J.C., Izumi, Y. and Bradley, E.F. (1971) Flux-profile relationships in the atmospheric boundary layer. J. Atmos. Sci., 28, 181-189.
- Bodin, S. (1979) A predictive numerical model of the Atmospheric Boundary Layer based on the turbulent energy equation. SMHI-report no. RMK 13, Norrköping, Sweden.
- Bøhler, T. and Isaksen, I.S.A. (1984) The atmospheric significance of liquid phase oxidation of SO₂ to sulphate by O₃ and H₂O₂. In: Physico-chemical behaviour of atmospheric pollutants.²B². Versino and G. Angeletti, Eds. Dordrecht, Reidel, 554-564.
- Christensen, O. and Prahm, L.P. (1976) A pseudospectral model for dispersion of atmospheric pollutants. J. Appl. Meteor., 15, 1284-1294.
- Eliassen, Anton and Saltbones, J. (1975) Decay and transformation rates for SO₂ as estimated from emission data, trajectories and measured air² concentrations. Atmos. Environ., 9, 425-429.
- Eliassen, Anton and Saltbones, J. (1983) Modelling of long-range transport of sulphur over Europe: A two-year model run and some model experiments. Atmos. Environ., 17, 1457-1473.
- Eliassen, Arnt and Hellevik, O. (1975) The design of a numerical model atmosphere with isentropic coordinate surfaces. Institute report series, no. 13, Institute for Geophysics, University of Oslo, Norway. 25 pp.
- Fox, D.G. and Orzag, S.A. (1973) Pseudospectral approximation to two-dimensional turbulence. J. Comput. Phys., 11, 612-619.

- Jacobs, C.A., Pandolfo, J.P. and Atwater, M.A. (1974) A description of a general three dimensional numerical simulation model of a coupled air-water and/or air-land boundary layer. IFYGL, Final report, CFM, Rep. No. 5131-509a, Center for the Environment and Man, Hartford, Conn., 85 pp.
- Kondratyev, J. (1969) Radiation in the atmosphere. Academic press, 912 pp. 187-202.
- Krishnamurti, T.N., Kanamitsu, M., Godbole, R., Chang, C.B., Carr, F. and Chow, J. (1976) Study of a monsoon depression (II), Dynamic structure. J. Meteor. Soc. Japan, 54, 208-225.
- Kuo, H.L. (1965) On formation and intensification of tropical cyclones through latent heat release by cumulus convection. J. Atmos. Sci., 22, 40-63.
- Kuo, H.L. (1974) Further studies of the parameterization of the influence of cumulus convection on large scale flow. J. Atmos. Sci., 31, 1232-1240.
- Louis, J.F. (1979) A parametric model of vertical eddy fluxes in the atmosphere. Boundary Layer Meteorol., 17, 187-202.
- Mesinger, F. and Arakawa, A. (1976) Numerical methods used in atmospheric models, Vol. 1, GARP publication series, no. 17, WMO, Geneva, 64 pp.
- OECD (1979) The OECD programme on long range transport of air pollutants. Measurements and findings, second action. OECD, Paris, France. (\approx 280 pp.)
- Pickard, G.L. (1970) Descriptive Physical Oceanography, Pergamon Press, 200 pp.
- Rohde H. and Isaksen, I.S.A. (1980) Global distribution of sulphur compounds in the troposphere estimated in a height latitude transport model. J. Geophys. Res., 85, 7401-7409.
- Semb, A. (1985) Circumpolar SO₂ emission survey. NILU OR 69/85, Lillestrøm, Norway.

Smolarkiewicz, P.K. (1983) A simple positive definite advection scheme with small implicit diffusion. Mon. Wea. Rev., 111, 479-486.

Sundqvist, H. (1981) Prediction of stratiform clouds: Results from a 5-day forecast with a global model. Tellus, 33, 242-253.

NORSK INSTITUTT FOR LUFTFORSKNING (NILU)
 NORWEGIAN INSTITUTE FOR AIR RESEARCH
 POSTBOKS 64, N-2001 LILLESTRØM

RAPPORTTYPE OPPDRAGSRAPPORT	RAPPORTNR. OR 82/86	ISBN-82-7447-762-9	
DATO JANUAR 1987	ANSV. SIGN. 	ANT. SIDER 63	PRIS kr 50.00
TITTEL A Model for Long Range Transport of Sulphur Dioxide and Particulate Sulphate in the Atmosphere - A Technical Description.		PROSJEKTLEDER T. Iversen	
		NILU PROSJEKT NR. O-8515	
FORFATTER(E) T. Iversen		TILGJENGELIGHET A	
		OPPDRAGSGIVERS REF.	
OPPDRAGSGIVER (NAVN OG ADRESSE) BP International Ltd. ECC, Britannia House, Moore Lane London, EC 24 IBU, England			
3 STIKKORD (à maks. 20 anslag) Sulphur Long Range Transport Modelling			
REFERAT (maks. 300 anslag, 7 linjer)			

TITLE
ABSTRACT (max. 300 characters, 7 lines) This report contains a documentation of a numerical model for the calculation of long range transport of sulphur dioxide and particulate sulphate. The model is eulerian with several vertical layers (at least three). The vertical coordinate is potential temperature. The model is specially designed for modelling Arctic air quality.

* Kategorier: Åpen - kan bestilles fra NILU A
 Må bestilles gjennom oppdragsgiver B
 Kan ikke utleveres C